# AUTOMATION OF CAROTID ARTERY STENOSIS MEASUREMENT IN ULTRASOUND IMAGES USING IMAGE SEGMENTATION TECHNIQUE

Author
AREENA KHAN
Registration Number
NUST201463154MSMME62414F

Supervisor

DR. SYED IRTIZA ALI SHAH

DEPARTMENTOF BIOMEDICAL ENGINEERING AND SCIENCES

SCHOOL OF MECHANICAL & MANUFACTURING ENGINEERING

NATIONAL UNIVERSITY OF SCIENCES AND TECHNOLOGY

ISLAMABAD, PAKISTAN.

AUGUST, 2018.

# AUTOMATION OF CAROTID ARTERY STENOSIS MEASUREMENT IN ULTRASOUND IMAGES USING IMAGE SEGMENTATION TECHNIQUE

Author

AREENA KHAN

Registration Number

NUST201463154MSMME62414F

A thesis submitted in partial fulfillment of the requirements for the degree of MS Biomedical Sciences

Thesis Supervisor:

Dr. Syed Irtiza Ali Shah

Thesis Supervisor's Signature:_____

DEPARTMENT OF BIOMEDICAL ENGINEERING AND SCIENCES
SCHOOL OF MECHANICAL & MANUFACTURING ENGINEERING
NATIONAL UNIVERSITY OF SCIENCES AND TECHNOLOGY,
ISLAMABAD, PAKISTAN.

AUGUST, 2018.

# Thesis Acceptance Certificate

It is certified that the final copy of MS Thesis written by Areena Khan (Registration No. NUST201463154MSMME62414F), of SMME (School of Mechanical & Manufacturing Engineering) has been vetted by undersigned, found complete in all respects as per NUST statutes / regulations, is free of plagiarism, errors and mistakes and is accepted as partial fulfilment for award of MS/MPhil Degree. It is further certified that necessary amendments as pointed out by GEC members of the scholar have also been incorporated in this dissertation.

Signature: _____

Name of Supervisor: Dr. Syed Irtiza Ali Shah

Date: _____

Signature (HOD): _____

Date: _____

Signature (Principal): _____

Date: _____

# EXAMIANTION COMMITTEE

We hereby recommend that the dissertation prepared under our supervision by: AREENA KHAN, NUST201463154MSMME62414F. Titled: "AUTOMATION OF CAROTID ARTERY STENOSIS IN ULTRASOUND IMAGES USING IMAGE PROCESSING TECHNIQUES" be accepted in partial fulfillment of the requirements for the award of Masters of Science in Biomedical Sciences degree with (___ grade).

| | |
|---|---|
| Committee Chair: Dr. Nosheen, HOD<br>SMME | Dated: |
| Committee Member: Dr. Umar Ansari, Lecturer<br>SMME | Dated: |
| Committee Member: Dr. Adeeb Shehzad, Assiatant Professor<br>SMME | Dated: |
| Supervisor: Dr. Syed Irtiza Ali Shah, Associate professor<br>SMME | Dated: |

_____ _____

(Head of Department) (Date)

## COUNTERSIGNED

Dated: _____ _____

(Dean / Principal)

# Declaration

I certify that this research work titled "*Automation of carotid artery stenosis measurement in ultrasound images using image segmentation techniques"* is my own work. The work has not been presented elsewhere for assessment. The material that has been used from other sources has been properly acknowledged / referred.

Signature of Student

AREENA KHAN

NUST201463154MSMME62414F

# Plagiarism Certificate (Turnitin Report)

This thesis has been checked for Plagiarism. Turnitin report endorsed by Supervisor is attached.

Signature of Student

AREENA KHAN

NUST201463154MSMME62414F

Signature of Supervisor

# Copyright Statement

# Acknowledgements

I am thankful to my Creator Allah Subhana-Watala to have guided me throughout this work at every step and for every new thought which You setup in my mind to improve it. Indeed, I could have done nothing without Your priceless help and guidance. Whosoever helped me throughout the course of my thesis, whether my parents or any other individual was Your will, so indeed none be worthy of praise but You.

I am profusely thankful to my beloved parents who raised me to this level and continued to support me throughout in every field of my life.

I would also like to express special thanks to my supervisor Dr. Syed Irtiza Ali Shah for his help throughout my thesis and also for teaching us Signals and Images in Medicine. I can safely say that I haven't learned any other engineering subject in such depth than the ones which he has taught.

I would also like to pay special thanks to Zaid Ahsan Shah for his tremendous support and cooperation. Each time I got stuck in something, he came up with the solution. Without his help I wouldn’t have been able to complete my thesis. I appreciate his patience and guidance throughout the whole thesis.

I would also like to thank Ahmed Raza, Saad Habib Qureshi, Zaeem Hadi, Maryam Shahid Rana, Javairia Yousaf, Amber Zahoor, Maria Javed, Ayesha Ambreen, Sameen Naz and Najwa Farooq for being on my thesis guidance and express my special Thanks to Dr. Nabeel Anwar for his help.

Finally, I would like to express my gratitude to all the individuals who have rendered valuable assistance to my study.

*Dedicated to Allah Almighty, my supportive parents and my teacher Mr. Zaid Ahsan Shah whose tremendous support, guidance and cooperation led me to this wonderful accomplishment.*

# Abstract

Atherosclerosis is one of the foremost cause of cerebrovascular diseases like heart attack and stroke worldwide. Accurate measurement of IMT and detection of carotid artery plaques in ultrasound images is crucial in the early diagnosis of these pathologies. Manual measurement of IMT and percentage carotid artery stenosis in hospital setups are more error prone due to user interaction and speckle noise in ultrasound images that eventually degrades the image resolution leading to inaccurate measurement of risk indicators of stroke. Recently, a few image processing techniques are used to avoid shortcomings of manual measurement of IMT and carotid artery plaque by medical experts. In this study, an automated segmentation technique for carotid artery plaque from ultrasound images is presented. B-mode gray scale ultrasound images are used to detect the plaque based on the algorithm as image acquisition, feature enhancement, artery wall matching, artery width (distance) matching, artery wall selection and enhancement, bounded distance map and determining carotid artery stenosis. Experimental results on 26 longitudinal images show the accuracy of the proposed method with the aid of medical expert's reports. Further, the proposed method does not need user interaction in all cases. The proposed technique will be further evaluated on larger database and stenosis from transverse images of carotid artery can also be measured.



Keywords: Carotid artery stenosis, Lumen detection, Plaque detection, Image segmentation, Distance Mapping.

# Table of Contents

Thesis Acceptance Certificate ..... iii
Declaration ..... v
Plagiarism Certificate (Turnitin Report) ..... vi
Copyright Statement ..... vii
Acknowledgements ..... viii
Table of Contents ..... xi
List of Figures ..... xiii
List of Tables ..... xvi
List of Acronyms ..... xvii
Chapter 1: INTRODUCTION AND LITERATURE REVIEW ..... 1
1.1 INTRODUCTION ..... 1
1.2 BACKGROUND ..... 1
1.2.1 Anatomy of Carotid artery ..... 1
1.2.2 Carotid Artery Disease ..... 2
1.2.3 Atherosclerosis ..... 2
1.2.4 Types of plaque ..... 4
1.2.5 Imaging of Carotid Artery Stenosis ..... 6
1.2.6 Ultrasonography ..... 7
1.3 LITERATURE REVIEW ..... 10
1.3.1 Active contour techniques ..... 12
1.3.2 Other segmentation techniques ..... 15
Chapter 2: METHODOLOGY ..... 17
2.1 Image Acquisition ..... 17
2.2 Feature Enhancement ..... 18
2.2.1 Local Thresholding ..... 18
2.2.2 Image segmentation ..... 18
**2.2.2.1 Edge Detection** ..... 18
2.2.3 Lines Enlisting ..... 20
2.3 Pairwise Matching ..... 21
2.4 Distance Matching ..... 24
2.5 Artery Width Selection ..... 27
2.6 Artery Walls Selection ..... 29
2.6.1 Artery Walls Detection ..... 29
2.6.2 Artery Walls Enhancement ..... 31
2.7 Lumen Width Detection ..... 32
2.7.1 Bounded Threshold Image ..... 32

2.7.2 Distance Map ..... 33
2.7.3 Lumen Centre Detection ..... 33
2.7.4 Bounded Distance Map ..... 34
2.8 Carotid Artery Stenosis Measurement ..... 35
Chapter 3: BENEFITS AND LIMITATIONS ..... 37
3.1 Benefits ..... 37
3.2 Limitations ..... 37
3.3 Medical Aspects ..... 37
Chapter 4: RESULTS AND DISCUSSION ..... 38
4.1 Results ..... 38
4.1.1 Statistical Data Analysis ..... 42
4.2 Discussion ..... 46
Chapter 5: CONCLUSION AND RECOMMENDATIONS ..... 47
5.1 Conclusion ..... 47
5.2 Future Recommendations ..... 47
Chapter 6: REFERENCES ..... 48

# List of Figures

**Figure 1.1:** Origin of Common Carotid Artery (CCA) (Molinari et al., 2010a) ..... 2
**Figure 1.2:** Sagittal view of a carotid artery containing plaque(Loizou, 2005)..... 3
**Figure 1.3:** (a) Type I plaque (b) Type II Plaque (c) Type III Plaque (d) Type IV Plauqe (e) Type V plaque (Loizou, 2005)..... 5
**Figure 1.4:** Scheme depicting the estimated diameter measures(Rouco, Azevedo, & Campilho, 2016). ..... 7
**Figure 1.5:** Ultrasound machine (a) ATL HDI-3000, (b) ATL HDI-5000 (Loizou, 2005) ..... 8
**Figure 1.6:** Ultrasound image of the CCA and demonstration of the IMC and plaque at the distant wall of the CCA, the lumen diameter, and the maximal stenosis (Loizou, 2014)..... 9
**Figure 1.7:** Ultrasound Sagittal Brightness approach image of a fine CCA(Molinari et al., 2010a)..... 9
**Figure 1.8:** B-mode grayscale ultrasound carotid artery image showing artery wall interfaces at near and far wall (Gutierrez et al., 2002)..... 13
**Figure 1.9:** Enhancement of near and far wall boundaries (Gutierrez et al., 2002)..... 14
**Figure 2.1:** Carotid Artery Stenosis Measurement Algorithm Flowchart..... 17
**Figure 2.2:** Threshold image..... 18
**Figure 2.3:** Four possible vertical pixel pair combinations in threshold image. ..... 19
**Figure 2.4:** Example (a) Threshold Image, (b) Up Lines Image, (c) Down Line Image. ..... 19
**Figure 2.5:** (a) Up Lines Image showing upper edges/lines (b) Down Lines Image showing down edges/lines..... 20
**Figure 2.6:** (a)Up Lines Image as example (b) One dimensional “Up Line Lengths” storing the lengths of upper lines (c) Three dimensional “Up Line Points”. ..... 21
**Figure 2.7:** Pairwise Matching Matrix showing 0 for valid pairs and 1 for invalid pairs..... 22
**Figure 2.8:** Zoomed portion of image showing invalid pairs having intersecting lines..... 22
**Figure 2.9:** Up line (u2) and Down line (d1) constitute as invalid pair shown in Pairwise Matching Matrix. ..... 23
**Figure 2.10:** Up edge/line (u1) and Down edge/line (d1) as an invalid pair..... 23
**Figure 2.11:** Condition of valid pair..... 24
**Figure 2.12:** Distance Matching Matrix. ..... 25
**Figure 2.13:** (a) Valid pair (b) Common Band matrix (c) Height differences matrix..... 26

**Figure 2.14:** Distance Matching Matrix showing the flagging of distances vs column numbers. ..... 26
**Figure 2.15:** Resultant single column and transpose. ..... 27
**Figure 2.16:** Test Image containing Up and Down edge lines ..... 28
**Figure 2.17:** Distance Vs Column Frequency Plot. ..... 28
**Figure 2.18:** ±5 Pixel band showing maximum number of columns per possible Artery Width. ..... 29
**Figure 2.19:** (a) Upper-Edges satisfying the artery width (b) Lower-Edges satisfying the artery width. ..... 30
**Figure 2.20:** (a) Upper-Edges satisfying the artery width (b) Number of white pixels in every row. ..... 30
**Figure 2.21:** Frequency plot of Number of white pixels Vs Row number for Down edges (blue) and Up Edges (Red). ..... 31
**Figure 2.22:** (a) Lower Artery wall→ Upper-Edges (b) Upper Artery wall→ Lower-Edges. ..... 31
**Figure 2.23:** (a) Lower Artery Wall Dilated (b) Upper Artery Wall Dilated. ..... 32
**Figure 2.24:** (a) Lower Artery Wall Image (b) Upper Artery Wall Image. ..... 32
**Figure 2.25:** (a) Mask of carotid artery (b) Bounded Threshold Image. ..... 33
**Figure 2.26:** (a) Threshold Image (b) Distance Map. ..... 33
**Figure 2.27:** (a) Threshold Image (b) Distance Map showing Lumen Centre location and intensity values. ..... 34
**Figure 2.28:** (a) Threshold Image (b) Bounded Distance Map. ..... 34
**Figure 2.29:** (a) Unbounded Threshold Image (b)Unbounded Distance Map ..... 35
**Figure 4.1:** (a) Original B-mode grayscale carotid artery ultrasound image (b) Threshold image. ..... 39
**Figure 4.2:** (a) Up Lines Image (b) Down Lines Image. ..... 39
**Figure 4.3:** Detected Up and Down edges. ..... 39
**Figure 4.4:** (a) Lower Artery wall (Upper-Edges) (b) Upper Artery Wall (Lower-Edges). .. 40
**Figure 4.5:** (a) Lower Artery Wall (b) Upper Artery Wall. ..... 40
**Figure 4.6:** Bounded Distance Map. ..... 40
**Figure 4.7:** Plot of Image Columns Vs Plaque Width in Artery. ..... 41
**Figure 4.8:** Plot of Image Column Vs Artery Stenosis Percentage. ..... 41
**Figure 4.9:** Comparison of manual and automatic carotid artery stenosis measurement. ..... 42

**Figure 4.10:** Original B-mode grayscale images and their Resultant images detected lumen (green) and plaque (red). ..... 44

# List of Tables

**Table 1.1** Overview of image processing techniques for segmentation of lumen and carotid plaques..... 12
**Table 4.1:** Statistical analysis of data. ..... 42
**Table 4.2:** Bar Graph showing automatic Vs manual measurement for lumen detection. ..... 45
**Table 4.3:** Bar Graph showing automatic Vs manual measurement for plaque detection. .... 45

# List of Acronyms

| | |
|---|---|
| **IMT** | Intima Media Thickness |
| **CCA** | Common Carotid Artery |
| **LI** | Lumen Interface |
| **MA** | Media Adventitia |
| **USG** | Ultrasound |
| **DMM** | Distance Matching Matrix |
| **PMM** | Pairwise Matching Matrix |
| **DM** | Distance Map |
| **B-mode** | Brightness mode |

# Chapter 1: INTRODUCTION AND LITERATURE REVIEW

## 1.1 INTRODUCTION

IMT measurement and detection of carotid artery plaques are the main predictors of stroke, manually measured by medical experts that are prone to human error. The objective of this thesis is to make a robust automated algorithm to accurately measure percentage carotid artery stenosis and provide early diagnosis leading to preemptive treatment for patients.

## 1.2 BACKGROUND

Stroke is the third leading cause of death having 9 % incidence of death worldwide. Carotid artery stenosis is main source of stroke as well as the 3$^{rd}$ major reason of demise worldwide (Loizou, 2005).

### 1.2.1 Anatomy of Carotid artery

Two Common Carotid arteries (CCA), one on each side of the neck, are the main arteries that provide blood to the neck, face and brain. Right Common Carotid artery (RCCA) emerges from Brachiocephalic trunk while Left Common Carotid artery (LCCA) emerges directly from the Arch of Aorta. Each Common Carotid artery (CCA) cleaves into External and Internal carotid artery. Internal Carotid artery (ICA) ascends towards the skull and supply the brain. While External Carotid artery gives blood to face, scalp, neck and tongue (Santos et al., 2013). Carotid sinus / bulb is the widened portion of Common Carotid artery exactly at its bifurcation level. Carotid artery is composed of 3 layers: (i) intima, the innermost layer, (ii) media, the middle layer and (iii) adventitia, the outermost layer. The intima is mainly composed of endothelium that is followed by the sub-endothelial layer of connective tissue having a covering of elastic fibers. This layer of artery wall is the one that is in direct contact with the lumen of artery containing blood. The middle layer (media) consists of muscular cells. While the adventitia is connective tissue and elastic fiber layer (Molinari, Zeng, & Suri, 2010a).

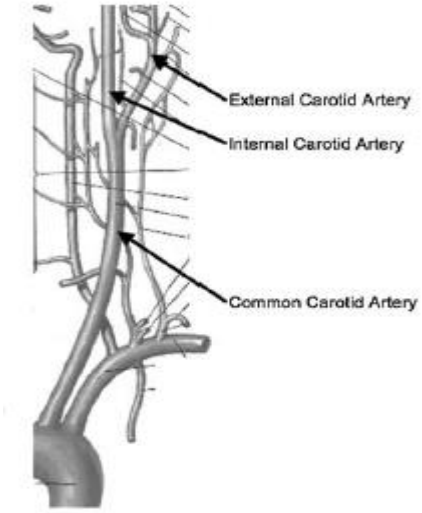


**Figure 1.1:** Origin of Common Carotid Artery (CCA) (Molinari et al., 2010a)

### 1.2.2 Carotid Artery Disease

Interruption or blockage of blood supply to brain caused by narrowing of artery leads to occurrence of stroke. There are two types of stroke (i) Ischemic stroke: caused by narrowing of artery leading to blockage or obstruction in the blood flow. (ii) Hemorrhagic stroke: artery stenosis causes the blood vessel to rupture (Gutstein & Fuster, 1999). Two types of risk factors contribute in stroke, non-modifiable ones are age, gender, race and family history while hypertension, diabetes, hyperlipidemia, cardiac disease, smoking, transient ischemic attacks (TIA's) etc. are modifiable risk factors (A. Nicolaides et al., 2003).

### 1.2.3 Atherosclerosis

The most common disease occurring in Common Carotid artery (CCA) is atherosclerosis or carotid stenosis. Atherosclerosis is the degeneration and thickening of the arterial wall due to accumulation of lipid and cholesterol deposits involving the intima and media, called as plaque which causes hardening or narrowing of artery lumen. It reduces blood flow (Zarins, Xu, & Glagov, 2001) (L. Christodoulou, Loizou, Spyrou, Kasparis, & Pantziaris, 2012a) and blood pressure that can initiate myocardial infarction, stroke and peripheral diseases normally called as cardiovascular diseases (CAD) (Yang et al., 2011). So, these diseases can be prevented by the early detection of plaque and percentage carotid artery stenosis measurement (Loizou, 2005). In atherosclerosed blood vessel, blockage to normal blood flow is due to the growing regions on the intimal layer of artery walls, this, in turn, leads to high blood pressure. As the

percentage of artery stenosis increases, it, in turn, increases the risk of stroke (Dis, 1995). It is assessed by measurement of carotid artery stenosis (P M Rothwell & Goldstein, 1995). The severity of stenosis is determined by the measurement of Intima-media thickness (IMT) and plaque thickness (Loizou, 2005). Certain predisposing factors are responsible for stroke such as age, gender, ethnicity, race, family history, diabetes, hypertension, heart disease, smoking and Transient Ischemic Attack (TIA) (A. Nicolaides et al., 2003). The risk marker and risk indicator of cardiovascular diseases is the Intima-media thickness (IMT) and measurement of percentage carotid stenosis. Intima-media thickness (IMT) holds some benefits as (i) the most initial sign to show the progress of atherosclerosis (ii) it can be repeatedly measured (iii) it can be measured non-invasively (Molinari et al., 2010a). The IMT is interpreted for instance the gap amid lumen–intima junction (LI) and the media–adventitia junction (MA) (Loizou, 2014).

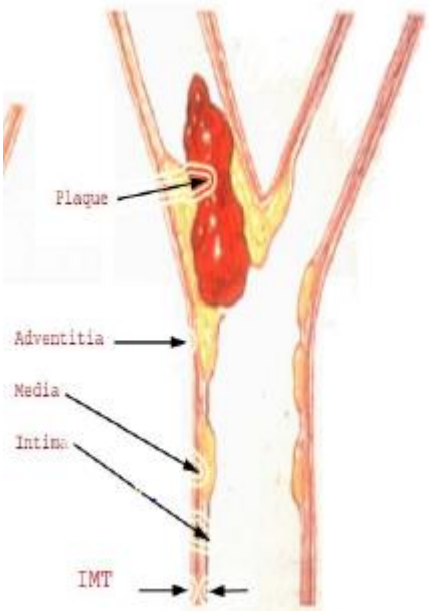


**Figure 1.2:** Sagittal view of a carotid artery containing plaque(Loizou, 2005).

### 1.2.4 Types of plaque

Plaques must be characterized according to their composition and structure in order to prevent these high risk plaques to cause heart attacks and strokes (C. I. Christodoulou, Pattichis, Pantziaris, & Nicolaides, 2003), (Middleton & Damper, 2004) (Zarins et al., 2001). There are two types of plaque (i) Stable or homogenous texture plaques that appear echogenic having smooth, irregular surface and bright echoes while (ii) Unstable or heterogeneous texture plaques are considered as those having irregular surface and less echoes (C. I. Christodoulou et al., 2003), (Geroulakos, Hobson, & Nicolaides, 1996) which mainly contribute in creating neurological problems (Wilhjelm et al., 1998), (El-Barghouty, Nicolaides, Bahal, Geroulakos, & Androulakis, 1996).

Plaques are also classified into two types:

1. **Calcified / Hard plaques**
   These plaques appear hyperechoic (more echoes) producing posterior acoustic shadowing in ultrasound images.
2. **Non-calcified / soft plaques**
   These plaques appear hypoechoic (mix echoes) in ultrasound images (Johnson, Kennelly, Decesare, Morgan, & Sparrow, 1985).

According to another classification, there are five types of carotid plaques given as:

1. **Type I Echo-lucent plaques:** These plaques consist of lipid content. Usually invisible in B-mode images but identified through blood flow Doppler images.
2. **Type II Predominantly echo-lucent plaques:** These plaques have less than 50 % echogenic areas.
3. **Type III Predominantly echogenic plaques:** Such plaques contain less than 50 % echo-lucent areas.
4. **Type IV Echogenic plaques.**
5. **Type V Calcified plaques.**

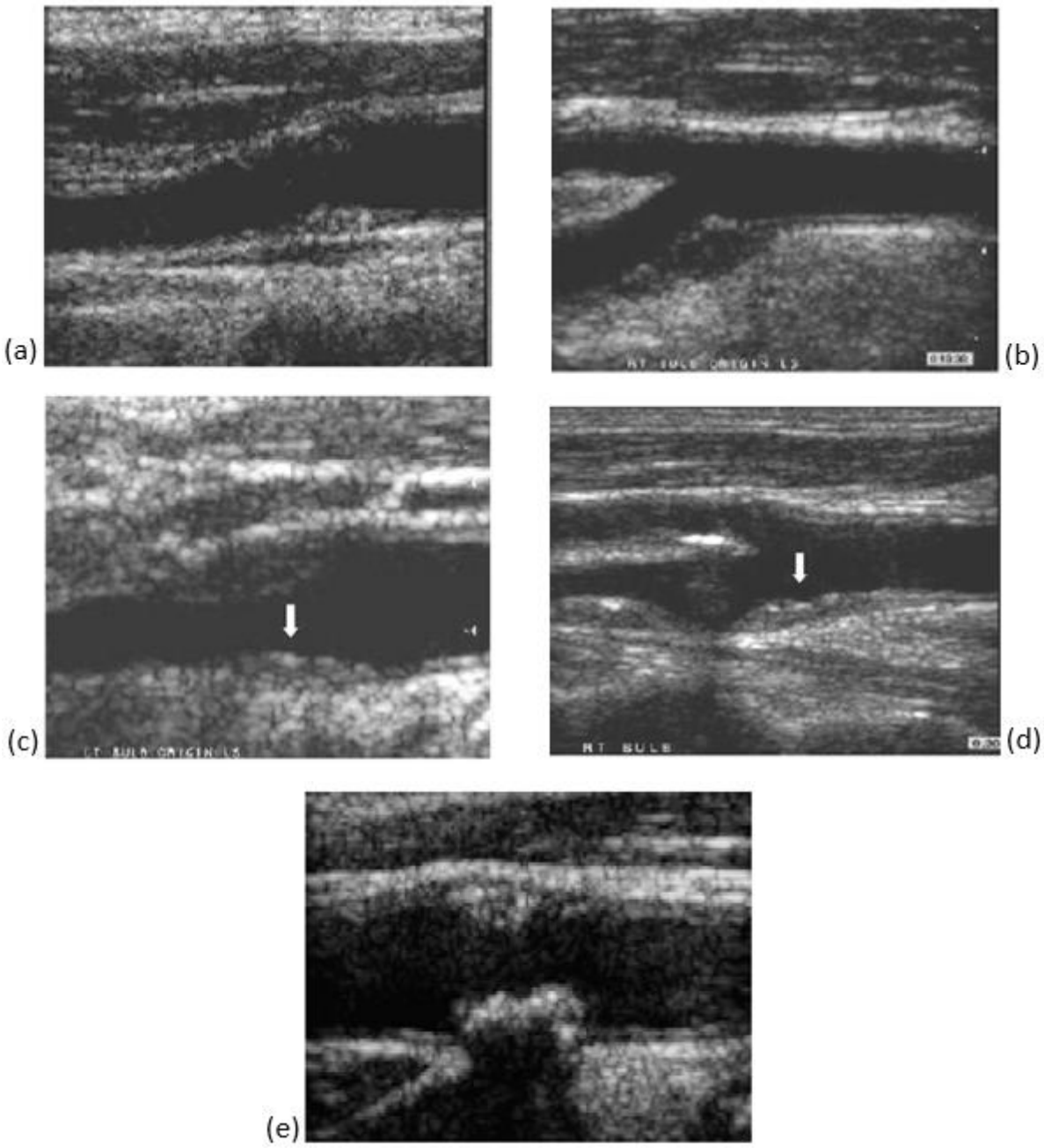


**Figure 1.3:** (a) Type I plaque (b) Type II Plaque (c) Type III Plaque (d) Type IV Plauqe (e) Type V plaque (Loizou, 2005).

Several studies conducted in different countries around the world such as Japan (Watanabe, Yamane, Egusa, & Kohno, 2004), China (Liu et al., 2008), United States (Bhuiyan, Srinivasan, Chen, Paul, & Berenson, 2006; Roman et al., 2006), America (Schargrodsky et al., 2008), Asia / Africa and Middle East and Europe (Pierre Jean Touboul et al., 2007) showed the importance of intima-media complex (IMC) as the risk mark of stroke / other cardiovascular diseases

(CVD). According to these studies, IMT exceeding 0.9-1.0 mm thickness is considered noteworthy enough to show the increased risk for occurrence of cardiovascular diseases (CVD). Some research studies showed that the intima-media thickness (IMT) increases with age and process of atherosclerosis can start even from childhood. In the younger age from 5 to 20 years, there might be an increase in intima-media complex (IMC) without causing atherosclerosis of artery. While in elderly people, the change in intima-media thickness (IMT) can also change the endothelium of artery that, in turn, increases the risk of stroke / cardiovascular diseases (CVD) (Fernhall & Agiovlasitis, 2008). Increased IMT is the indication of level of rate of stenosis which shows the distance between the layers of artery walls containing atherosclerotic plaques. Therefore, computation of intima-media thickness and identification of carotid arterial stenosis is an important predictor of stroke (Peter M Rothwell et al., 1994).

### 1.2.5 Imaging of Carotid Artery Stenosis

To prevent the occurrence of stroke, imaging modalities like X-ray Angiography, CT Angiography, Ultrasound Imaging and Magnetic Resonance Angiography (MRA) are used to evaluate the status of carotid arteries and to quantify the intima-media complex (IMC) (Loizou, 2005). Advantages of producing high resolution, sharper and cross-sectional images made CT scan and MRI superior to Ultrasound but it is preferred to image the carotid arteries to detect and characterize the plaques, to measure intima-media width, diameter of lumen & degree/percentage of artery stenosis (P. J. Touboul et al., 2007). Two types of radiations are used in Radiology to examine the internal structures of human body. Ionizing radiations that consist of high energy particles or rays causing ionization in the medium and are harmful. Non-ionizing radiations, on the other hand, are not harmful. Out of all imaging modalities, Ultrasound and MRI use non-ionizing radiations. Ultrasound has most important advantage of using mechanical sound waves (non-ionizing) and can also be easily used for follow up of patients for monitoring the status of disease. MRI also uses non-ionizing radiofrequency waves but it is not commonly used for assessing the carotid artery features as it is expensive and at times, requires the introduction of contrast agent that in rare cases, might cause side effects (Boussel et al., 2007)

Percentage of reduction of artery lumen diameter relative to normal vessel reference diameter is called as percentage or degree of artery stenosis. According to the definition of NASCET

study (Committee, 1991), percentage carotid artery stenosis is calculated as "the variance between the maximum and minimum region of the artery as compared to the maximum region (A. Nicolaides et al., 2003) (A. N. Nicolaides, Kakkos, Griffin, Geroulakos, & Bashardi, 2002)" shown by the following formula,

$$100\left[1-\frac{dICA,min,}{dICA,distal}\right] \qquad (1.1)$$

$d_{ICA,min,}$ is the minimum diameter of Internal Carotid Artery(ICA) at the level of maximum stenosis/narrowing, while $d_{ICA,distal}$ is the diameter of maximum normal opening in the distal normal portion of ICA.

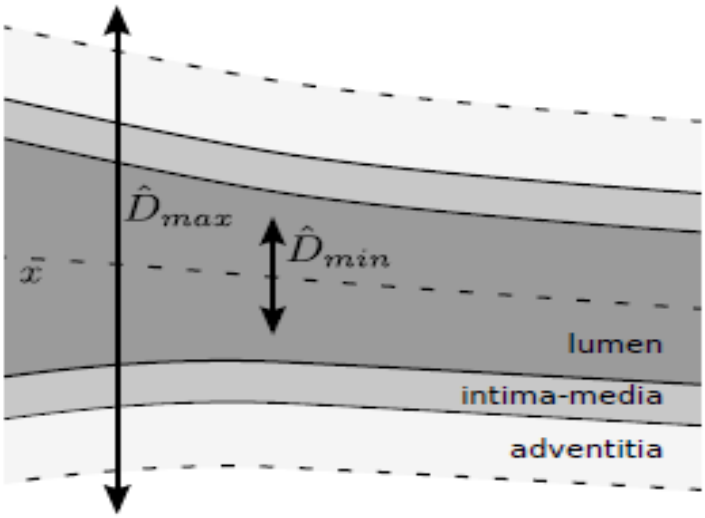


**Figure 1.4:** Scheme depicting the estimated diameter measures(Rouco, Azevedo, & Campilho, 2016).

### 1.2.6 Ultrasonography

Ultrasound is the most significant non-invasive investigation to rule out atherosclerosis in the carotid arteries. It sends sound waves with a frequency above 20,000 Hz that interacts with the tissue through reflection, transmission, refraction, attenuation and receives echoes to form an electronic image. It has many benefits because of its real time imaging, non-invasiveness, fast examination of patient, cost effectiveness, easy availability and safety to the patients in the aspect of having no harmful biological effects as it uses sound waves (Naik, Gamad, & Bansod,

2013). But ultrasound images have few short comings like poor resolution and low signal-to-noise ratio because of attenuation, speckle noise and acoustic shadowing giving rise to artifacts (Chaudhry, Hassan, Khan, & Kim, 2013). Speckle noise is an interference to the sound wave due to scattering (Molinari et al., 2010a). In addition, ultrasound imaging is also dependent on operator skills (Naik et al., 2013). Intra-observer variability is another limitation of ultrasound in which the same structure observed by same operator in different situation is different (Wendelhag, Liang, Gustavsson, & Wikstrand, 1997). Last but not the least, inter-observer variability also exists in ultrasound images (Jeremy D Gill, Ladak, Steinman, & Fenster, 2000), (Fetics et al., 2001). The intima-media width is manually measured by operator but because of this, it is time taking and not a reliable method.


**Figure 1.5:** Ultrasound machine (a) ATL HDI-3000, (b) ATL HDI-5000 (Loizou, 2005)

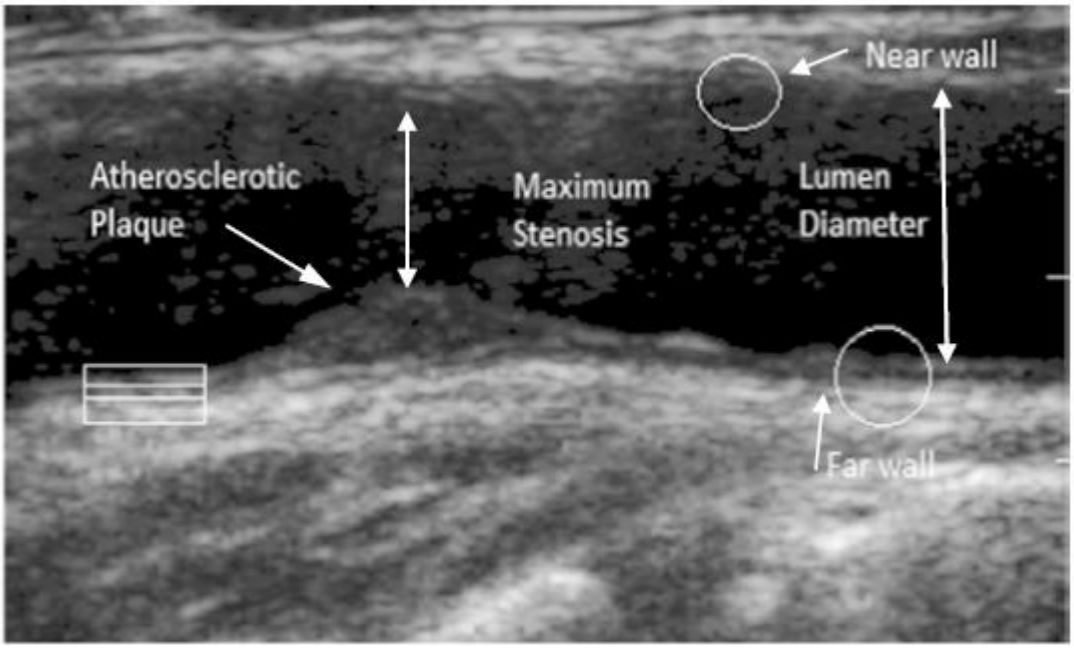


**Figure 1.6:** Ultrasound image of the CCA and demonstration of the IMC and plaque at the distant wall of the CCA, the lumen diameter, and the maximal stenosis (Loizou, 2014).

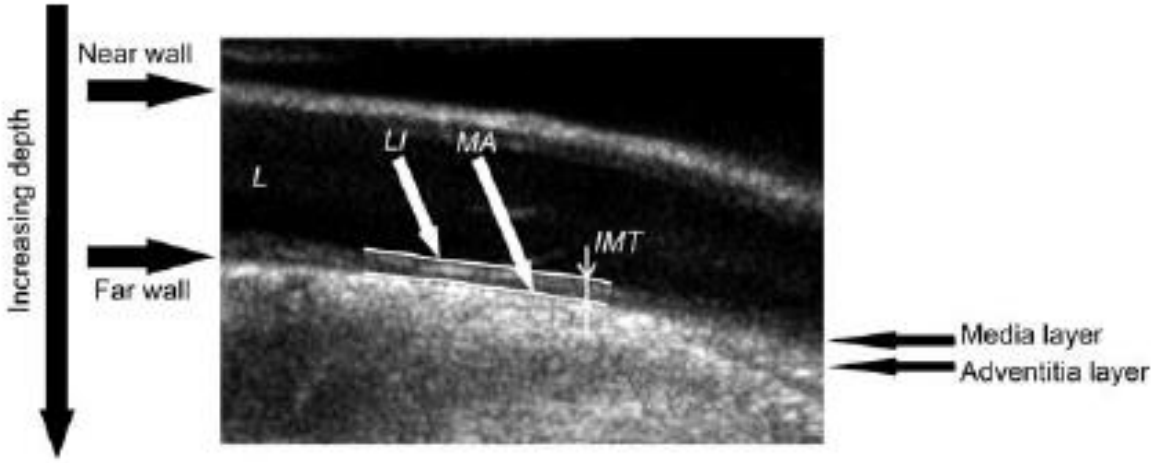


**Figure 1.7:** Ultrasound Sagittal Brightness approach image of a fine CCA(Molinari et al., 2010a).

## 1.3 LITERATURE REVIEW

The need for proposing Dynamic Programming techniques was the fact that due to the involvement of various operators, the manual measurement faced many variations in the studies. To overcome this problem, Gutavson (1997) tried four unique techniques, to be specific maximal gradient, Dynamic Programming (DP), mathematical prototype and balanced filter for segmentation of intima-media thickness (IMT) and lumen from one longitudinal ultrasound carotid artery image. The outcomes demonstrated that the Dynamic programming approach did superior to others in regard of robustness and border continuity, in spite of this fact, the borders could not be drawn effectively (Gustavsson, Abu-Gharbieh, Hamarneh, & Liang, 1997).

Another study showed that a star algorithm was proposed by Abolmaesumi (2000) to approximate the carotid artery center using transverse images and Kalman filter technique was used to roughly appreciate the carotid artery boundary. The carotid artery center could be distinguished by the star algorithm by taking into account it like the midpoint of gravity, however the outcomes were not extremely precise (Abolmaesumi, Sirouspour, & Salcudean, 2000).

A study done in 2000 by Jill, a semiautomatic technique was presented in order to follow the advancement of atherosclerotic carotid plaque in 3D images, through the use of Balloon model that was characterized by a triangle-shaped mesh/net. The net was physically introduced in the lumen of artery and after that pushed externally to the point when it achieved the wall by administering an expansion energy to mesh. The above mentioned technique was tested on two 3 dimensional unnatural carotid images produced from two distinctive vascular phantoms. The outcomes of this method demonstrated that segmentation was not precise as it was exceptionally tedious and borders were not properly drawn as well. In addition, manual correction and user interaction was impractical (J D Gill, Ladak, Steinman, & Fenster, 2000).

| Author | Year | Segmentation Technique | Segmented Area | Advantages | Limitations |
|---|---|---|---|---|---|
| Gutavson (Wendelhag et al., 1997) | 1997 | Dynamic Programming | IMT, artery lumen | Robust technique | Artery walls boundaries could not be drawn effectively. |
| Abolmaesumi (Liang, Wendelhag, Wikstrand, & Gustavsson, 2000) | 2000 | Star Kalman Filter | Carotid artery center | – | – |
| Jill (J D Gill et al., 2000) | 2000 | Balloon model | Carotid plaque | Applicable on 3D ultrasound carotid images | No satisfactory results, manual correction was needed. |
| Ladak (Ladak, Thomas, Mitchell, Rutt, & Steinman, 2001) | 2001 | Discrete dynamic contour | Artery wall and lumen | – | – |
| Zahalka (Zahalka & Fenster, 2001) | 2001 | Deformable model | Carotid artery lumen | – | – |
| Hamou (Hamou & El-Sakka, 2004) | 2004 | Canny Edge Detector | Carotid Plaque | No manual segmentation. | – |
| Gutierrez et al. (Gutierrez et al., 2002) | 2002 | Snake segmentation | Lumen diameter | Full automation | Not reliable in follow up studies for IMT changes |

| | | | | | |
|---|---|---|---|---|---|
| Christos P. Loizou et al. (L. Christodoulou, Loizou, Spyrou, Kasparis, & Pantziaris, 2012b) | 2012 | Adaptive snake-contour segmentation | CCA , plaque | _ | _ |
| A Chaudhry et al. (Chaudhry et al., 2013) | 2013 | Active contour | CCA | Reduced user interaction and snake has self-adaptive nature | Not applicable to plaque images |

**Table 1.1** Overview of image processing techniques for segmentation of lumen and carotid plaques

### 1.3.1 Active contour techniques

Fei Mao in 2000 detected the carotid artery lumen through deformable model. Manual interaction was the drawback of this study as the single seed point placement for the initialization of deformable model was done by a medical expert. To handle the speckle noise, artifacts, gaps, shadows and changes in shape of artery lumen, mathematical morphology operations and entropy map calculations was considered as important steps for initialization. The accuracy of this technique was significant but the seed point placement by expert involved intra-operator variability that made the technique semiautomatic (Mao, Gill, Downey, & Fenster, 2000).

Ladak (2001) (Ladak et al., 2001) proposed a discrete dynamic contour approach in order to segment the inner cavity of the artery and its wall in sagittal sonographic images of carotid artery, in which the primary snake shape was provided by the operator. After that, the contour was misshaped to adjust the innermost arterial wall boundaries. On every 2D carotid artery image, the segmentation was done and then a 3 dimensional spline surface was reproduced with limited component meshing from all 2 dimensional segmented profiles (Ladak, Milner, & Steinman, 2000) . This technique was tried on blood MRI images in which expert could alter

the final snake contour. Jill (Jeremy D Gill, Ladak, Steinman, & Fenster, 1999) (Jeremy D Gill et al., 2000) produced a same deformable model for 3D ultrasound carotid artery images in which the mesh was utilized to separate the final 3D boundary. The mesh, basically, was created from the finite element triangulation. In a study done by Zahalka et al. (2001), he developed a geometrically deformable approach for 3 dimensional transverse artery images by giving a seed point in the carotid artery cavity. In segmentation, three input parameters were needed by the snake and a contour variability was accounted there, because of the selection of the seed point (Zahalka & Fenster, 2001).

A study done by MA Gutierrez, in 2002, proposed a technique in order to measure intima media thickness and diameter of lumen by enhancing the artery wall boundary followed by **active contour technique.** The artery wall interfaces were manually detected for reference and adjusted in case of low resolution images by the manual operator and compared with the results obtained from automatic techniques (Gutierrez et al., 2002).

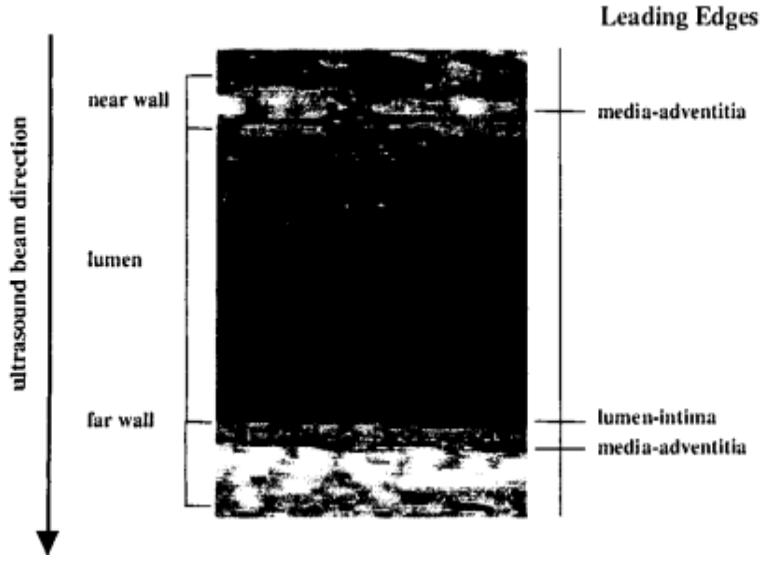


**Figure 1.8:** B-mode grayscale ultrasound carotid artery image showing artery wall interfaces at near and far wall (Gutierrez et al., 2002).

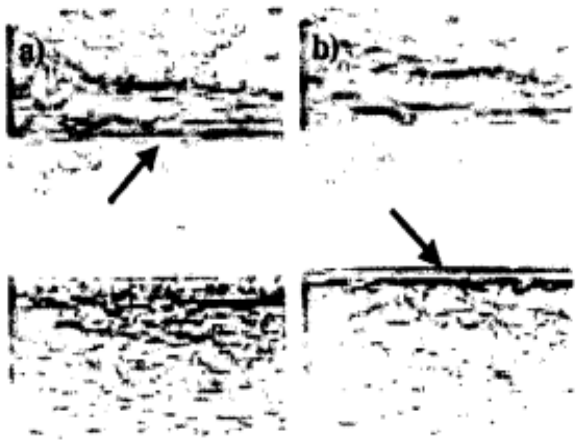


**Figure 1.9:** Enhancement of near and far wall boundaries (Gutierrez et al., 2002).

Measurement of intima-media thickness (IMT) and carotid artery stenosis are the main risk predictors for clinical evaluation of stroke. For evaluation of these significant markers, a full segmentation of CCA was done by Christos P. Loizou et al. (2012) that was based on adaptive snake-contour segmentation algorithm. This algorithm segmented the CCA into different regions that were IMT, intima-media (IL), medial-layer (ML), carotid lumen and plaque. Before the application of snake segmentation, image normalization, binarization and adaptive hybrid median filtering were done on the carotid artery images. The study concluded that level set segmentation and snake contour segmentation techniques showed better results with manual segmentation techniques (L. Christodoulou et al., 2012b).

A recent study done by A Chaudhry et al. (2013) presented active contour approach and classification techniques for sonographic carotid artery images. The study was done on 250 images (114 normal and 136 abnormal) of 38-78 years' age group patients. To avoid the rotation of ultrasound images during its acquisition a pre-processing tool "image alignment" was used. Normal and diseased carotid artery images were distinguished by Support vector machine (SVM) classification. A comparison of manual and automatic segmentation methods has also been done in this study. Concluding, the snake segmentation approach in this study reduced user interaction and provided accurate and early detection of carotid plaques (Chaudhry et al., 2013). The autonomous and self-adaptive nature of snakes made it superior to other image processing techniques.

### 1.3.2 Other segmentation techniques

C. I. Christodoulou et al. (2003) identified the asymptomatic carotid plaques that might cause stroke through multiple texture feature and multiple classifiers using self-organizing map (SOM) classifier and statistical (K-nearest neighbor) KNN classifier that classified the carotid plaque as symptomatic and asymptomatic. In this study. region of interest (ROI) containing plaque was identified and outlined manually by expert (C. I. Christodoulou et al., 2003).

A study done by Hamou AK et al. (2004) proposed a segmentation technique using Canny edge detector in order to segment the carotid artery plaques. The study was done to overcome the hindrance caused by speckle noise that prevented the proper detection of artery wall boundary and also the problem of poor angulation of probe while imaging the artery. The study started with histogram equalization of the gray levels of an image, followed by Canny edge detection that first smoothed the image through Gaussian filter and then extracted the edges. The third step was the morphological operation that filled the gaps and holes in the plaque. Boundary extraction was also applied using morphological operation. Last but not the least, the output image was overlaid on the original image. This algorithm prevented the need for involvement of manual measurement (Hamou & El-Sakka, 2004).

There are two different issues in performing segmentation of carotid artery images. One is the marking of region of interest (ROI) on which segmentation is needed to be performed. And the second is the differentiation of intima and media layers from the lumen of carotid artery containing blood. After this, the boundaries of intima-lumen (LI) and media-adventitia (MA) are extracted. Many segmentation techniques discussed previously have been introduced by researchers but most of them involved user interaction to some extent. But Silvia Delsanto et al. (2006) presented a study which identified echo lucent type II and echogenic plaques in the carotid walls of diseased patients and increased intima-media thickness (IMT) through Completely User-independent Layer Extraction (CULEX2) algorithm that preserved user-independence and pixel fuzziness in the ultrasound B-mode carotid artery images (Delsanto et al., 2006).

Another study done by Filippo Molinari (2010) introduced an integrated approach (Carotid artery layer extraction using an integrated approach [CALExia]) by combining certain steps as geometric feature extraction, line fitting and classification. This approach was able to automatically detect carotid artery walls by finding near and far wall adventitia layer in 200 longitudinal B-mode grayscale ultrasound images. It possessed three main advantages as (i) no

human interaction (ii) it was able to detect artery wall in normal as well as pathological images (iii) both near and far wall adventitia layer was extracted (Molinari, Zeng, & Suri, 2010b).

U. Rajendra Acharya et al. (2013) proposed a CAD system that accurately distinguished between symptomatic and asymptomatic carotid plaques in order to avoid unnecessary surgeries previously done in asymptomatic patients. The combination of trace transform and fuzzy texture techniques determined the textural differences in both classes of plaques using some grayscale features. The features extracted from outlined plaque regions trained some classifiers in order to classify new test plaques. Two databases of 146 (44 symptomatic to 102 asymptomatic) and 346 (196 symptomatic and 150 asymptomatic) images were used to test the respective CAD system. The classification accuracies of 93.1% and 85.3 % were obtained through this robust system. Low cost, easy application and non-invasive properties of this system can make it more applicable to the market (Acharya et al., 2013).

No study was done in the history on the segmentation of common carotid artery (CCA) bifurcation region except the one that introduced an integrated segmentation technique in ultrasound images. CCA at the level of bifurcation, was divided into various regions such as intima-media complex (IMC), artery lumen diameter and carotid plaque area. The technique was based on snake segmentation along with applying few steps before performing segmentation. The steps were image normalization, despeckle filter for removing noise, initial contour estimation and morphological operation. Manual measurement and correction could easily be done in this technique. Results showed the insignificant differences between manual measurement and snake segmentation (Loizou, Kasparis, Spyrou, & Pantziaris, 2013).

A study done by José Rouco et al. (2016) proposed a technique for detection of lumen centerline in longitudinal B-mode ultrasound images of carotid artery through the use of local symmetry analysis based on local phase information of dark pixels that increases the effectiveness of common carotid artery (CCA) lumen centerline. Symmetry, contrast features and location were used to analyze these candidates in 200 images. This approach was not affected by the speckle noise, artifacts and contrast of the image (Rouco et al., 2016).

# Chapter 2: METHODOLOGY

The overall algorithm consists of two major steps leading to measurement of percentage carotid artery stenosis which are artery wall detection and lumen width detection. The proposed methodology of fully automated carotid artery stenosis measurement algorithm consists of the following steps: image acquisition, feature enhancement, Artery wall detection, lumen width measurement and carotid artery stenosis measurement. The flowchart of this algorithm is shown below:

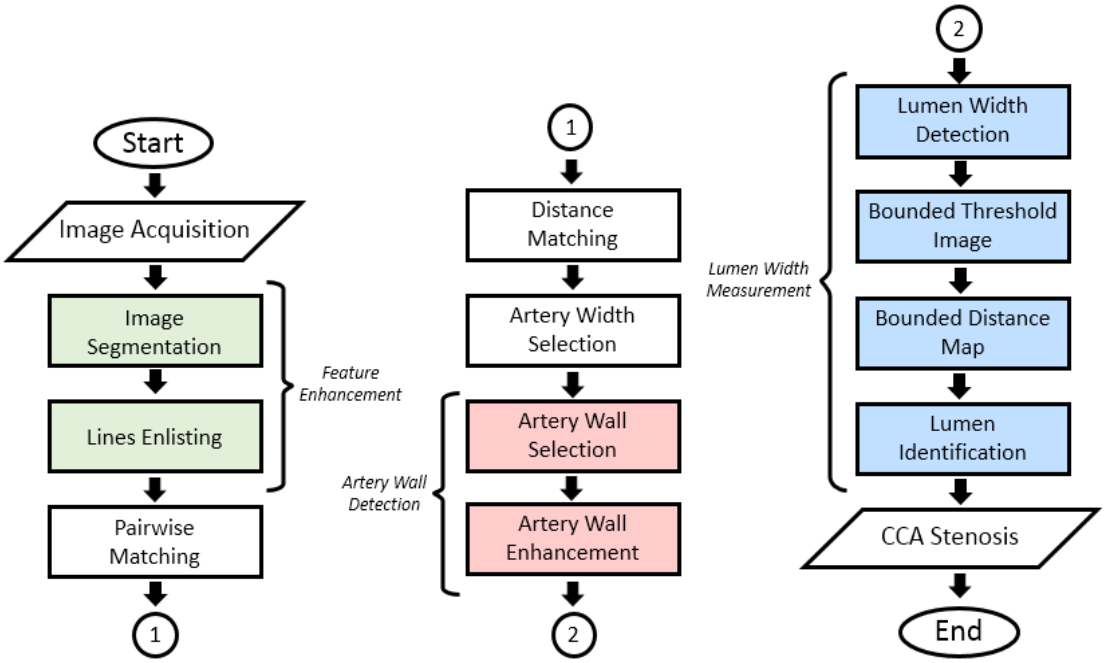


**Figure 2.1:** Carotid Artery Stenosis Measurement Algorithm Flowchart.

## 2.1 Image Acquisition

B-mode grayscale carotid artery images were acquired from the ultrasound scanner Toshiba Xario with the transducer having a frequency range of 5-7MHz, with the insonation plane perpendicular to the carotid artery in order to make its appearance horizontal from left to right side of ultrasound image. A total of 26 images (11 normal and 15 diseased) were used for this study. The images were cropped to remove the side markers, rulers, annotations and patient biodata. The images were resized to the dimensions of 200 x 400. All image segmentation steps were performed with Matlab R2017a.

## 2.2 Feature Enhancement

All RGB images were first converted to grayscale intensity images.

### 2.2.1 Local Thresholding

A process in which grayscale intensity image is converted to a binary image (black and white, pixel values 0 and 1 respectively).

Local thresholding was performed on all images. It estimates a different threshold value for each pixel according to the average intensity of neighboring pixels within a window of r radius. By using this thresholding, the images can be prevented from the effects of contrast or brightness that, in turn, reduces salt and pepper noise in the image without using median filter.

**Figure 2.2:** Threshold image.

### 2.2.2 Image segmentation

#### *2.2.2.1 Edge Detection*

The upper and lower edges/ lines were separately detected from the threshold images by generating two output images “Up Lines Image” and “Down Lines Image”. All vertical pixel pairs of the threshold image were checked one by one. There were four possible pixel combinations for all vertical pairs in the threshold image shown in the figure below:

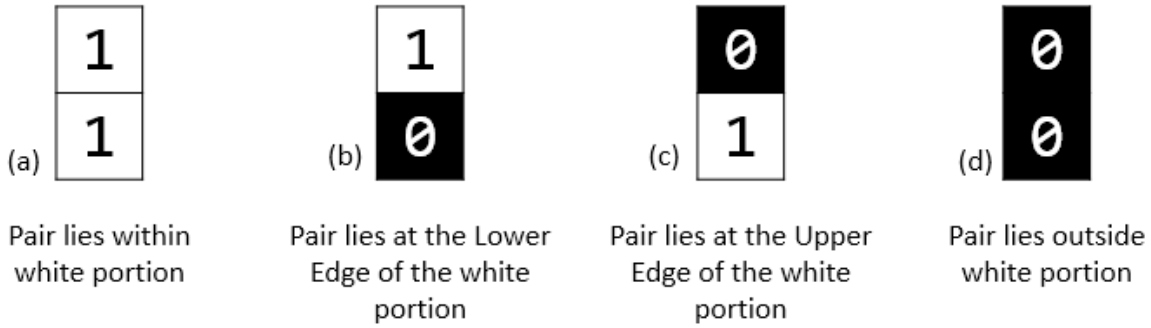


**Figure 2.3:** Four possible vertical pixel pair combinations in threshold image.

White portion in threshold image was set as a reference. If any edge lies below white portion, it was referred as Lower edge / line. While upper edge is the one that exists above the white portion in the threshold image.

Following were the conditions on the basis of which edges/ lines of the image were detected.

1. If, in any vertical pixel pair, a test pixel has intensity value greater than the pixel above it, as shown in Figure 12 (c), set the value of that pixel at exactly same location in the "Up Lines Image" as 1, shown in Figure 13 (b).
2. If the test pixel has intensity value greater than the pixel below it, as shown in Figure 12 (b), set the test pixel value at the same location in the "Down Lines Image" as 1 shown in Figure 13 (c).
3. While, put the pixel value 0 for both pixels in the "Up Lines Image" and "Down Lines Image", if vertical pixel pairs have combination shown in Figure 12 (a) and 12 (d) as pixel pair in (a) is white portion with no edges and pixel pair in (d) might be any lumen.

Consider the following example in the figure below.

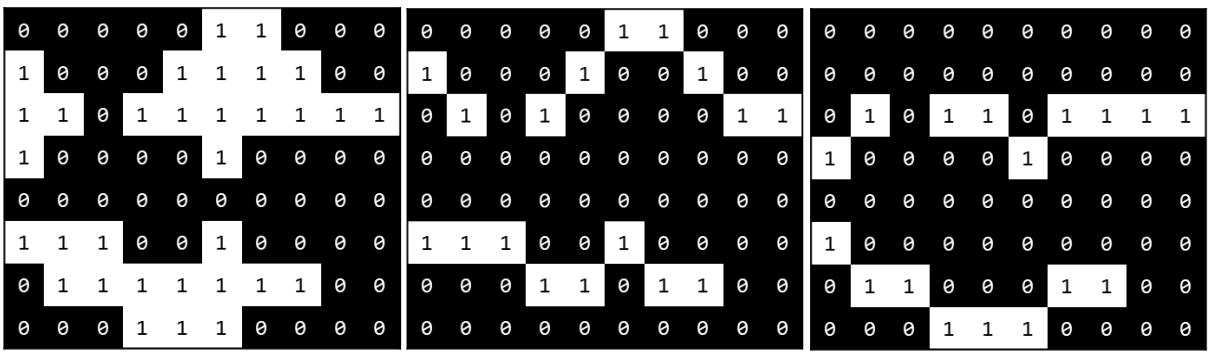


**(a)** **(b)** **(c)**

**Figure 2.4:** Example (a) Threshold Image, (b) Up Lines Image, (c) Down Line Image.

The white pixels were retained in the “Up Lines Image” and “Down Lines Image” respectively as shown in the Figure 14.

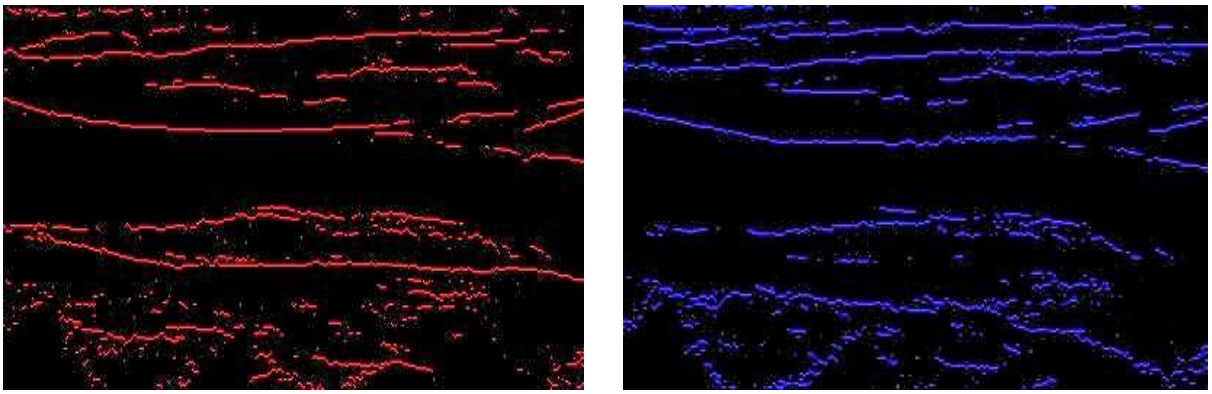

**(a)** **(b)**

**Figure 2.5:** (a) Up Lines Image showing upper edges/lines (b) Down Lines Image showing down edges/lines.

### 2.2.3 Lines Enlisting

“Up Line” and “Down Line Images” were used to populate *“Up Lines List”* and *“Down Lines List”* respectively. *“bwboundaries”* function was used to trace the exterior boundary of a line defining its contour by listing down the row and column coordinates of pixels in a binary image. “Up Line Points” and “Down Line Points” three dimensional matrices were generated that store the information of all upper and down edges/lines such as the front face of the three dimensional matrix shows row and column coordinates in two columns shown in Figure 15 (c). While the up and down lines are listed number wise in depth of three dimensional matrices respectively.

“Up Line Lengths” and “Down Line Lengths” one dimensional matrices were created that listed down the length of upper and down lines as values respectively. All lines having length less than four were removed to make the algorithm fast.

Consider the following example in Figure 2.6.

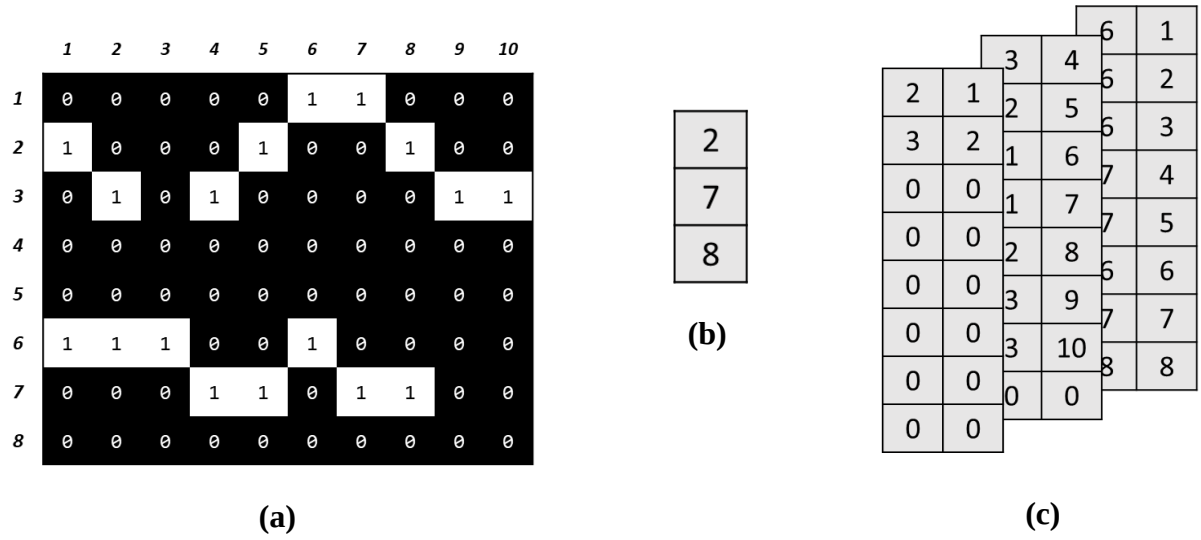


**Figure 2.6:** (a)Up Lines Image as example (b) One dimensional "Up Line Lengths" storing the lengths of upper lines (c) Three dimensional "Up Line Points".

## 2.3 Pairwise Matching

Artery wall detection and lumen width measurements are the two important parameters for measuring percentage carotid stenosis.

Pairwise Matching matrix was generated, initialized with zeros, that stores all the pairs which can be good candidates for reconstructing **"Artery Walls"**. The number of columns of this matrix was equal to the number of down lines while the number of rows was equal to the number of up lines. Both up and down lines were checked pairwise and marked as valid or invalid pairs in Pairwise Matching matrix according to the criteria mentioned. The Pairwise Matching Matrix shows ∅ for valid pairs and 1 for invalid pairs.

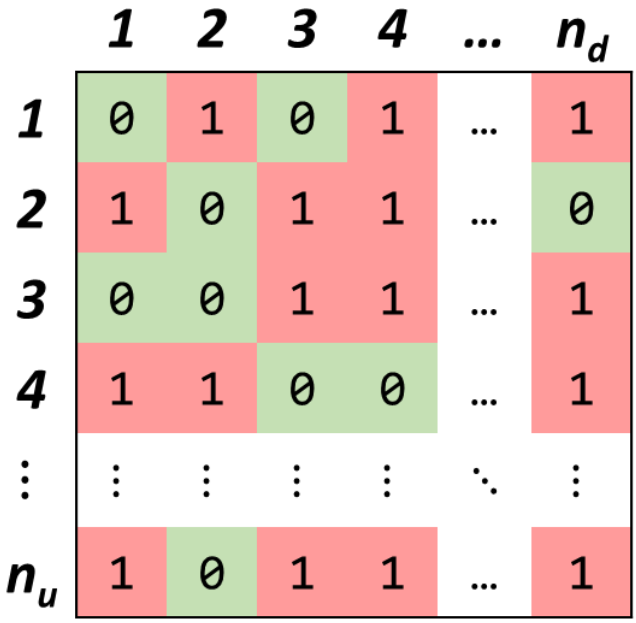


**Figure 2.7:** Pairwise Matching Matrix showing 0 for valid pairs and 1 for invalid pairs.

The criteria for ruling out invalid pairs in Pairwise Matching matrix are given as following:

1. A pair in which up and down lines are intersecting with each other at any common point was marked invalid pair in Pairwise Matching Matrix as artery is wide open with upper and lower wall maintaining a specified distance.

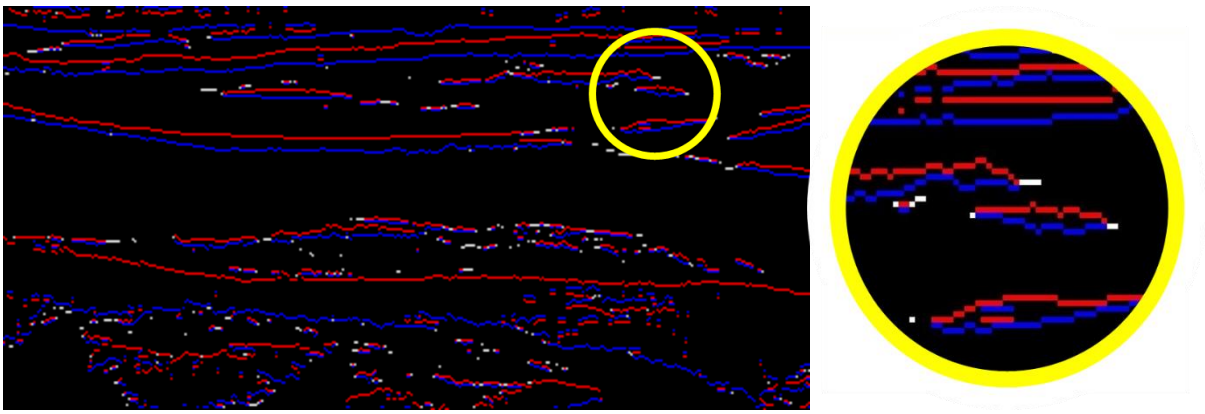

**Figure 2.8:** Zoomed portion of image showing invalid pairs having intersecting lines.

2. A pair of lines having no common columns constitute an invalid pair.

   For Example, in the Figure (), pairs having Up line (*u*1) and Down line (*d*1), Up line (*u*1) and Down line (*d*2), Up line (*u*2) and Down line (*d*2) are valid as they have common columns between them. While pair containing Up line (*u*2) and Down line (*d*1) has no common column, it was marked invalid in Pairwise Matching Matrix.

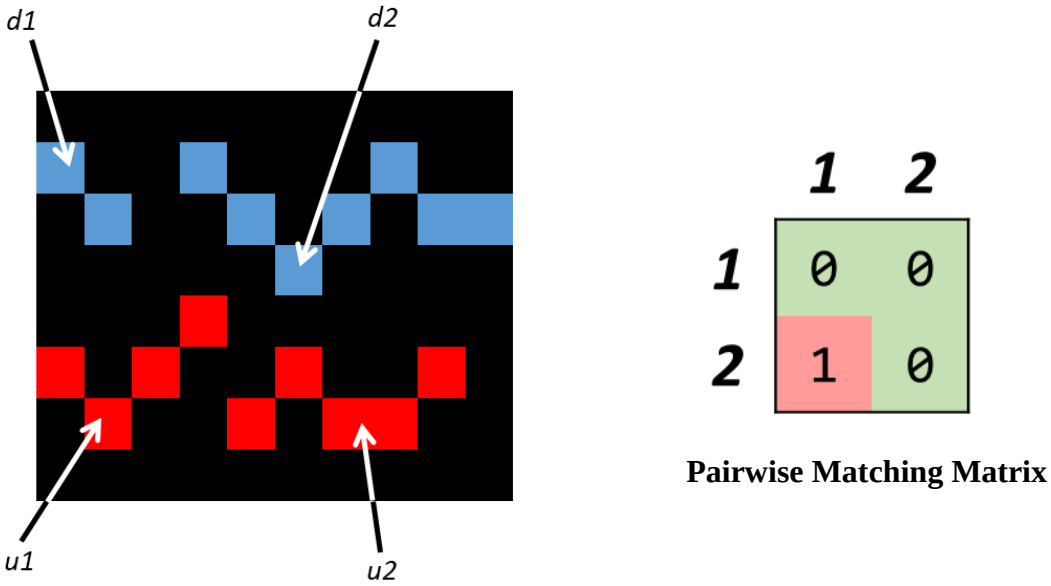


**Figure 2.9:** Up line (u2) and Down line (d1) constitute as invalid pair shown in Pairwise Matching Matrix.

3. A pair in which up edge is above the down edge and the one having down edge below up edge is an invalid pair as lumen of artery is sandwich between upper wall and lower wall having up edge below down edge.

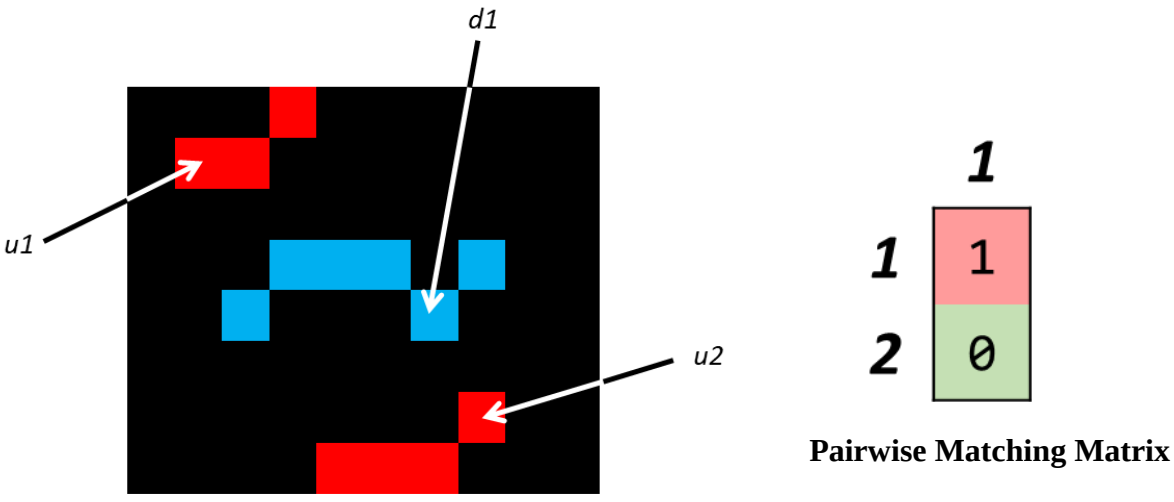


**Figure 2.10:** Up edge/line (*u*1) and Down edge/line (*d*1) as an invalid pair.

The validity of such pair was ensured by a condition that if the maximum Y (row) value (green line) of Up edge is greater than the minimum Y (row) value (yellow line) of Down edge, such pair is considered valid.

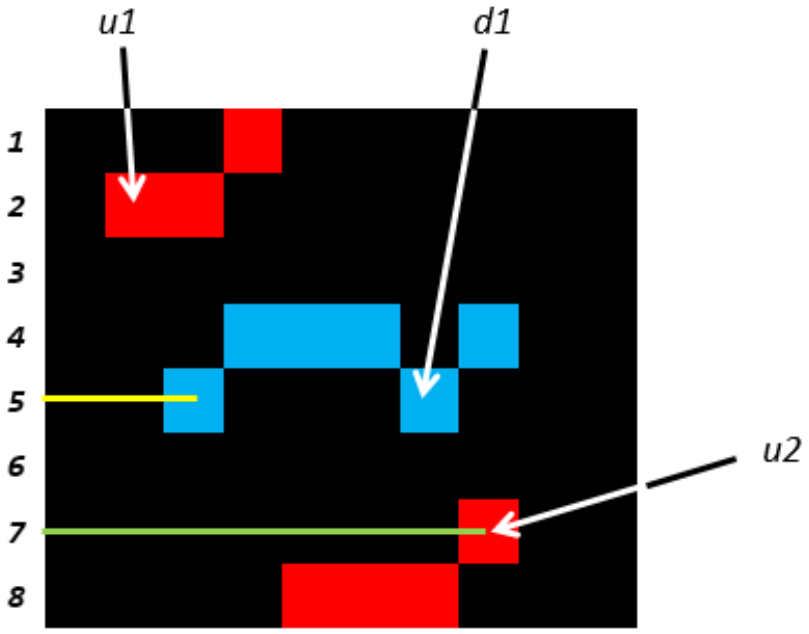


**Figure 2.11:** Condition of valid pair

All pairs that fulfilled above mentioned three criteria were marked as invalid pair while all others were considered valid pairs in Pairwise Matching Matrix.

## 2.4 Distance Matching

The Pairwise Matching Matrix (PMM) identified all the valid pairs which can potentially constitute ***'Artery Walls'***. A matrix called as Distance Matching Matrix (DMM) was generated that was initialized with zeros. The number of columns of this matrix was made equal to the number of columns of the original image (400 columns) while the number of rows was equal to the possible artery width or matching distances between up and down edges.

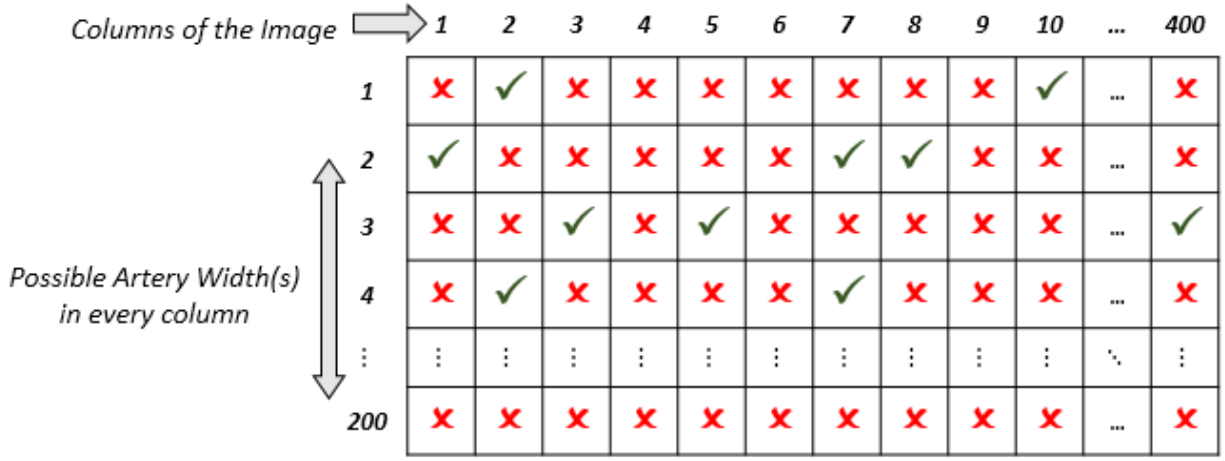


**Figure 2.12:** Distance Matching Matrix.

In order to generate the Distance Matching Matrix, all the valid pairs were checked one by one from Pairwise Matching Matrix.

1. Up and Down edge lines of one valid pair were extracted from Pairwise Matching Matrix.
2. The common band within that pair was determined that showed all the overlapping columns between Up and Down line. The column numbers of common band were stored in one dimensional "Common Band" matrix, shown in Figure 2.13 (b).
3. The height difference between the upper and down line within the Common Band was calculated and stored in another one dimensional "Artery Widths" matrix, shown in Figure 2.13 (c).

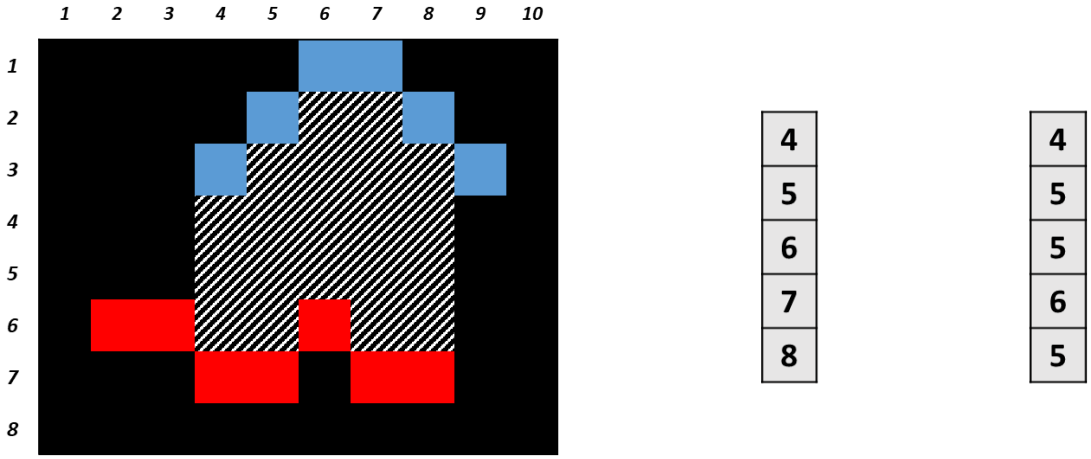


**Figure 2.13:** (a) Valid pair (b) Common Band matrix (c) Height differences matrix.

4. Flagging the appropriate location of the Distance Matching Matrix.

   4a. Column numbers were given by the "Common Band" Matrix.

   4b. Row numbers were given by the respective height differences.

The Distance Matching Matrix shows that which distance is satisfied at a specific column of Common Band shown in Figure 23.

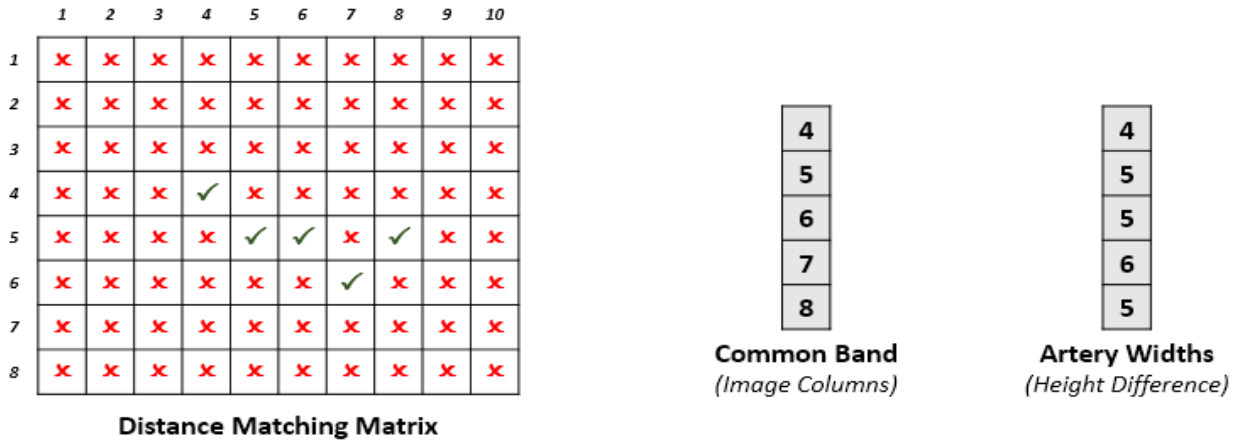


**Figure 2.14:** Distance Matching Matrix showing the flagging of distances vs column numbers.

## 2.5 Artery Width Selection

The Distance Matching Matrix was used to select the possible "Artery Width".

1. The Distance Matching Matrix contains 1 for ✓ and 0 for ×.
2. All the columns of the Distance Matching Matrix were added into a single column and the resultant was transposed to give the frequency plot that shows number of columns per possible ***'Artery Width'***.

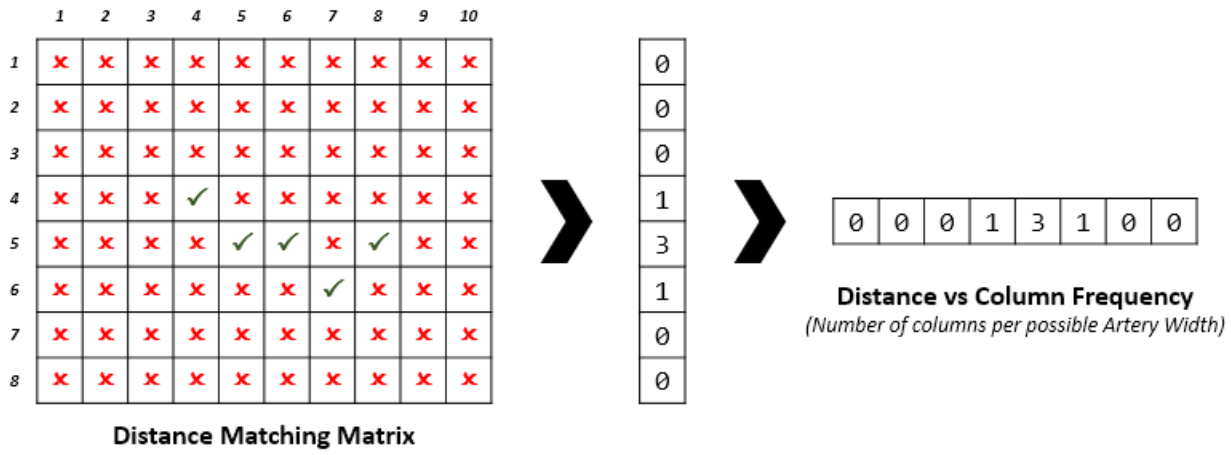


**Figure 2.15:** Resultant single column and transpose.

Figure 25 shows the test image and its frequency plot showing the number of columns at specific distances. For Example, in the frequency plot shown below, 85 columns are satisfying the distance (possible Artery Width) of 64 but as the artery cannot be dead straight containing a fix single distance between its upper and lower walls, a summation window of width 11 is swept across the Distance Vs Column Frequency, that averages the number of columns in the vicinity of 64 distance indicated by red colored plot and the resultant is stored at the center location of the window. The Artery Width value with the maximum average number of columns in the ±5 Distance vicinity is selected as the expected 'Artery Width.'

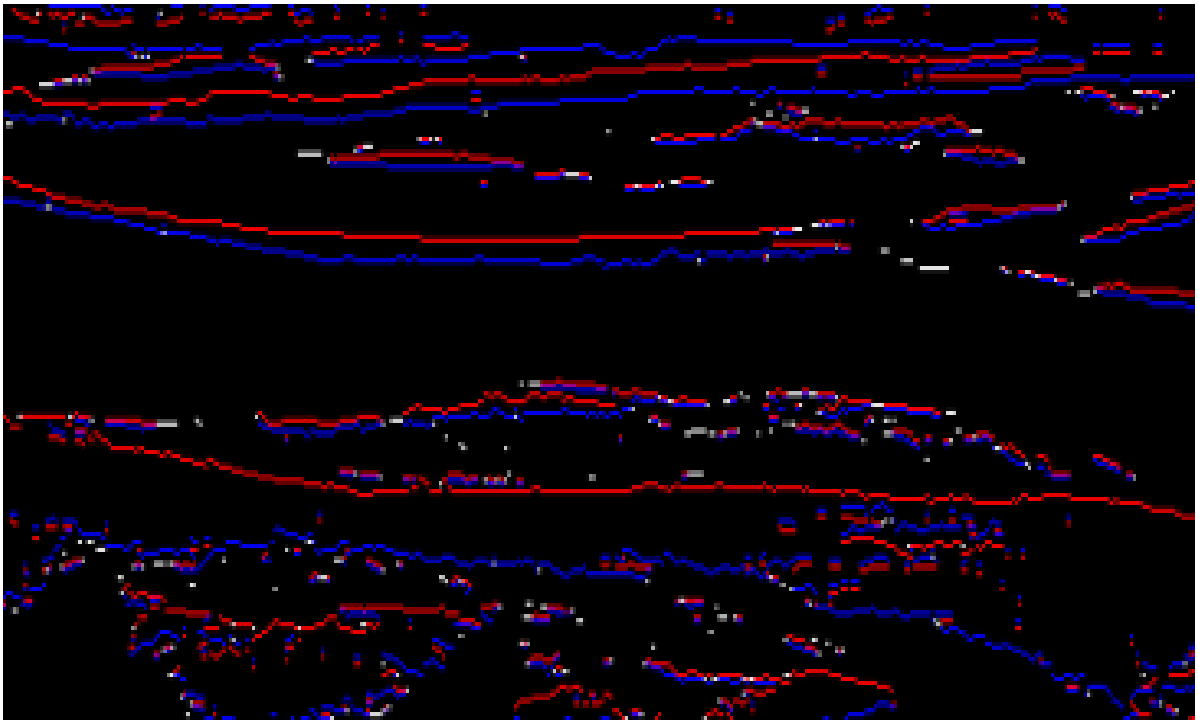

**Figure 2.16:** Test Image containing Up and Down edge lines

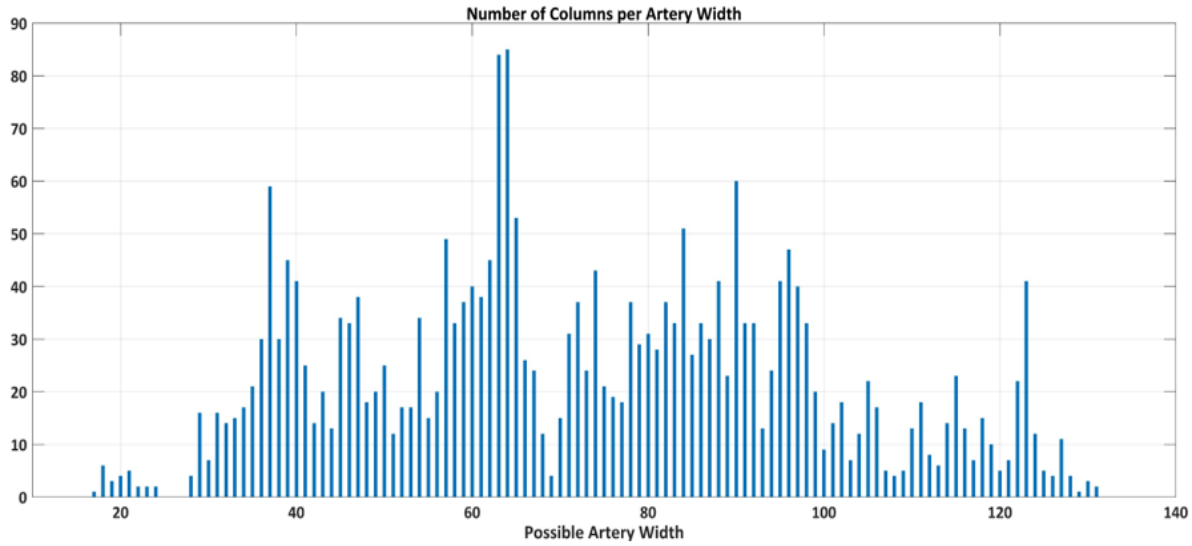


**Figure 2.17:** Distance Vs Column Frequency Plot.

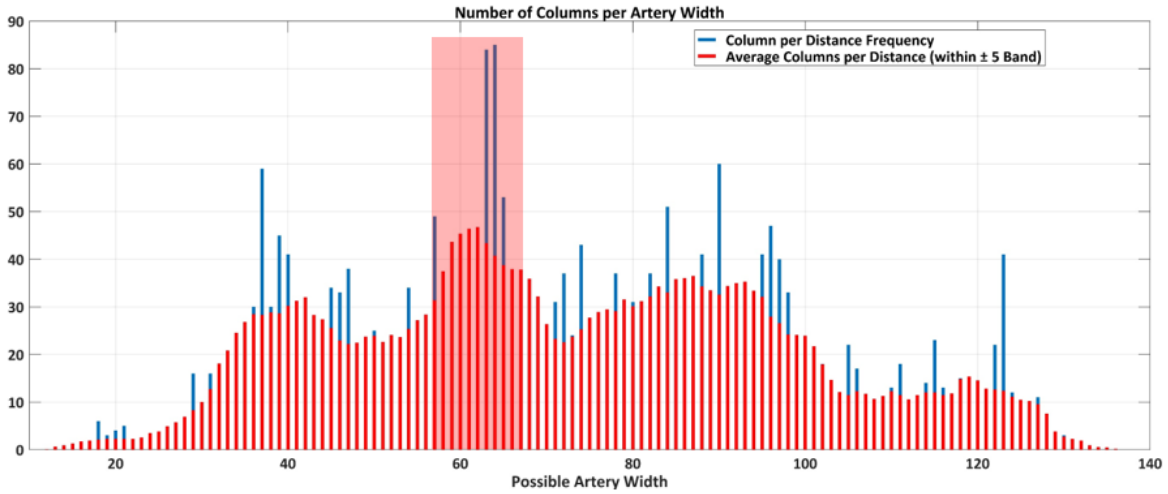


**Figure 2.18:** ±5 Pixel band showing maximum number of columns per possible Artery Width.

## 2.6 Artery Walls Selection

The next phase is to select artery walls using the up and down lines chosen in the previous steps.

### 2.6.1 Artery Walls Detection

The expected Artery Width is used to identify good candidates for the 'Artery Walls'.

For up-lines, good candidates are those which have at least one valid pair with down-lines, and that valid pair has the average vertical distance, within the expected Artery Width. The similar corollary holds for good candidates for down-lines.

***The Upper 'Artery Wall' will be composed of some of the 'Down-Lines' only and the Lower 'Artery Wall' will be composed of some of the 'Up-Lines' only.***

From all the Up and Down edges, only those edges which satisfied the Artery Width were kept and rest were removed that gave all those valid pairs which were good candidates for artery wall selection as shown in Figure 2.19.

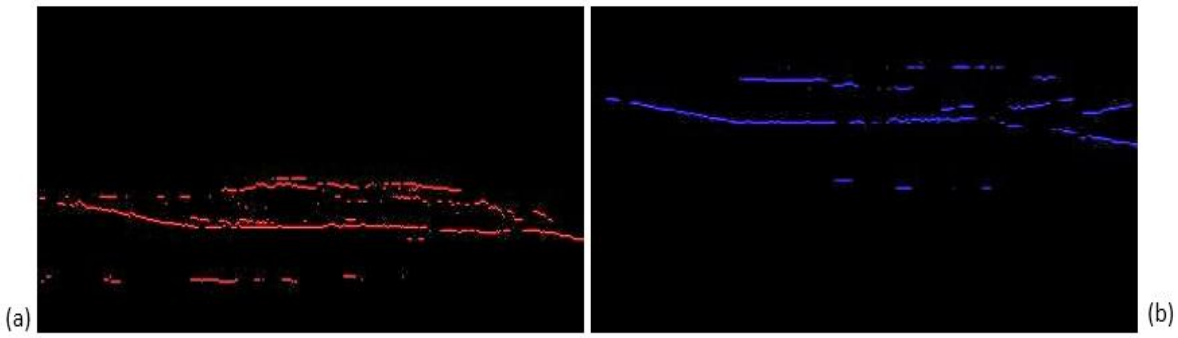


**Figure 2.19:** (a) Upper-Edges satisfying the artery width (b) Lower-Edges satisfying the artery width.

*Example of Up Edges:*

All the columns of the Up Edges Image were added into a single column and the resultant was transposed to give the frequency plot that shows number of white pixels per row.

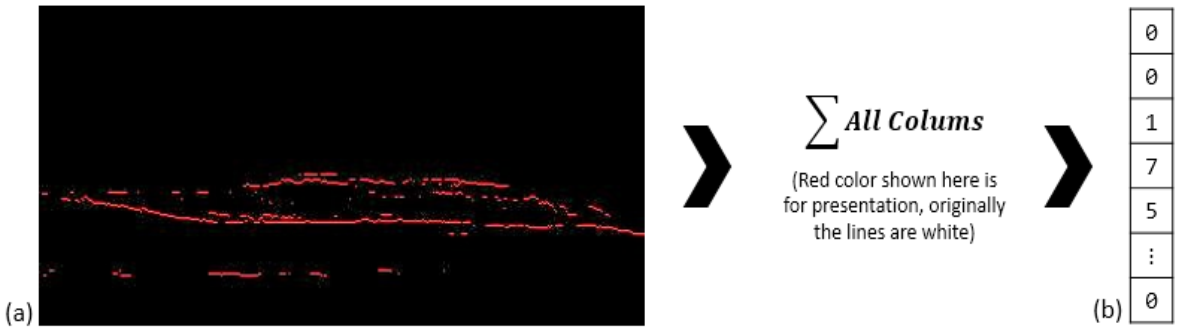


**Figure 2.20:** (a) Upper-Edges satisfying the artery width (b) Number of white pixels in every row.

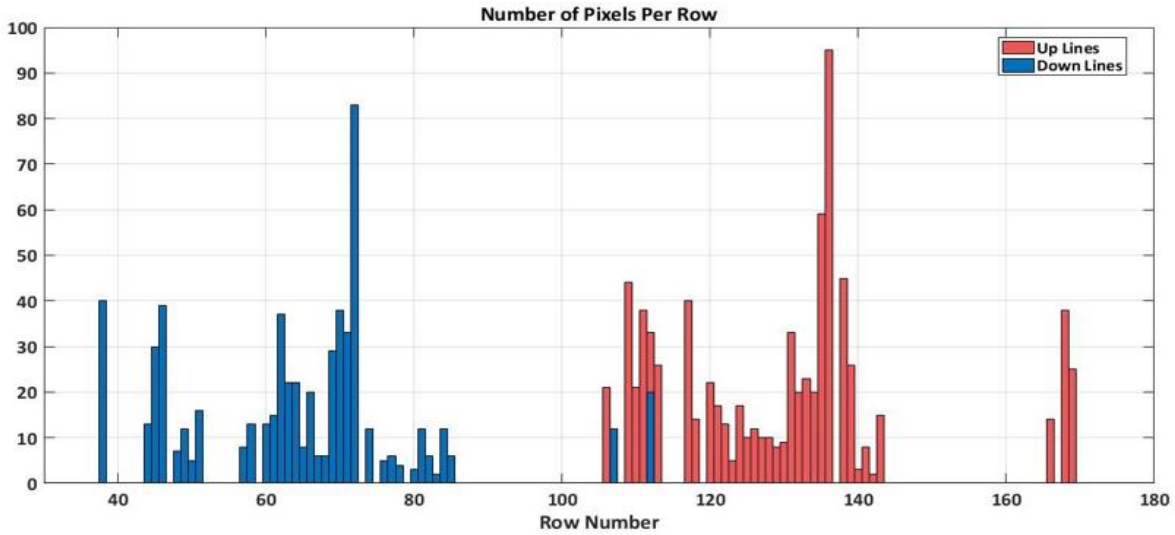


**Figure 2.21:** Frequency plot of Number of white pixels Vs Row number for Down edges (blue) and Up Edges (Red).

A ± 10 bound was selected having only those rows containing Down edges for making Upper wall and Up edges for making Lower wall of artery as shown in the Figure 31. The selected bounded rows resulted in the removal of further edges/ lines.

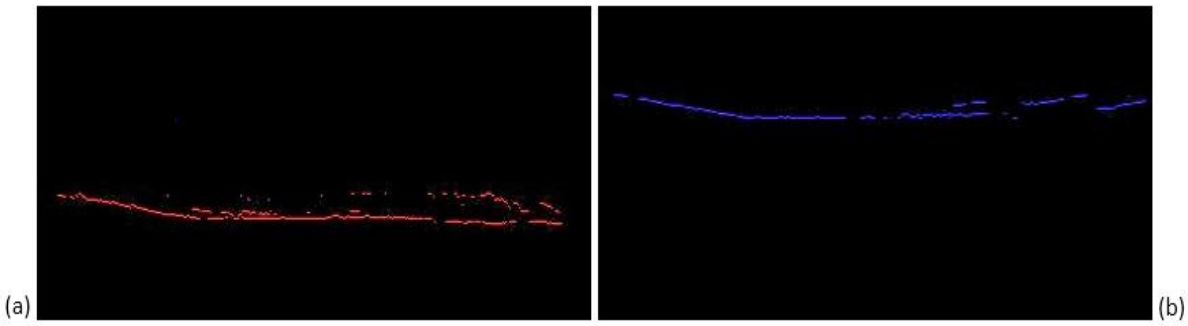


**Figure 2.22:** (a) Lower Artery wall→ Upper-Edges (b) Upper Artery wall→ Lower-Edges.

### 2.6.2 Artery Walls Enhancement

The final candidates for artery walls were dilated horizontally to cover all columns of the image. These dilated lines were then collapsed vertically to result in the upper and lower walls of the artery.

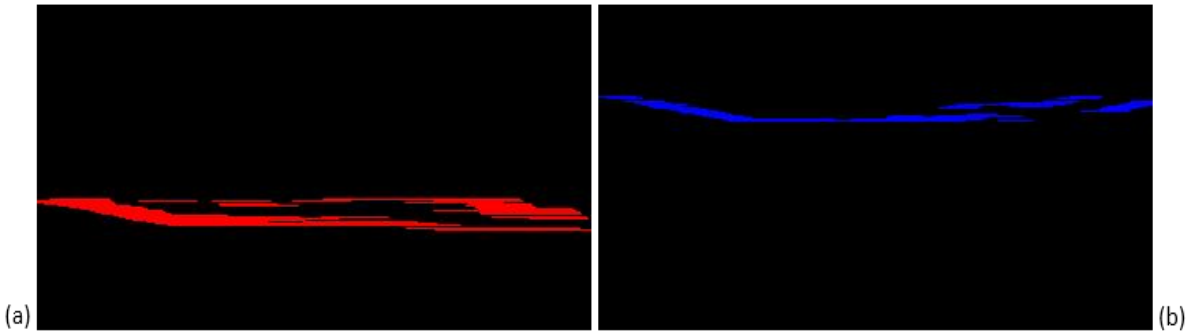


**Figure 2.23:** (a) Lower Artery Wall Dilated (b) Upper Artery Wall Dilated.

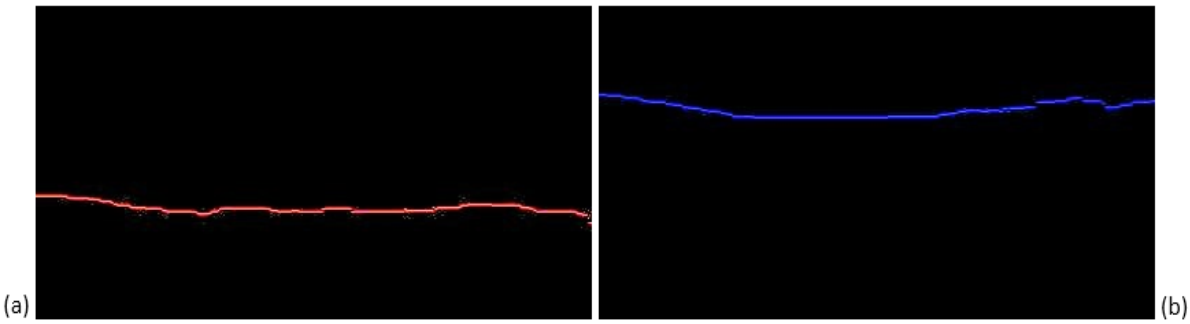


**Figure 2.24:** (a) Lower Artery Wall Image (b) Upper Artery Wall Image.

## 2.7 Lumen Width Detection

Now in order to determine the width of the lumen in every column the threshold image is bounded and subjected to the distance mapping filter.

### 2.7.1 Bounded Threshold Image

The Upper and Lower ***Walls*** of ***Artery*** were used to bound the threshold image, thus making an encapsulated artery within the threshold image. The pixels above the upper artery wall and the pixels below the lower artery wall were set as white by giving them intensity value 1. By doing this, a mask of artery was created after both the images were paired together and this mask was then overlaid on the threshold image thus creating a Bounded Threshold Image.


**Figure 2.25:** (a) Mask of carotid artery (b) Bounded Threshold Image.

### 2.7.2 Distance Map

The Distance Map function (***DistMap.m***) takes a binary image as an input and returns an output image. Every pixel location in the output image has the intensity value equal to the distance of the nearest white pixel, from that location, in the input image. The Distance Map is calculated by making concentric test circles of increasing radii. At radius 0, a pixel intensity value is checked, if it is 1 in input image, its value is set as 0 in output image and the algorithm moves to next pixel. The radius of the circle which encompasses a white pixel is set as the output intensity value for that location and the algorithm moves to the next pixel location. The Distance Map operates on all pixels.

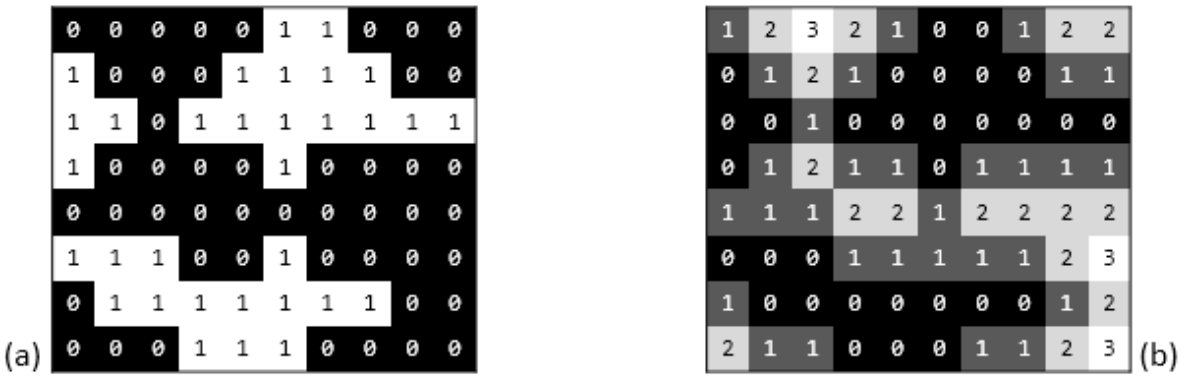


**Figure 2.26:** (a) Threshold Image (b) Distance Map.

### 2.7.3 Lumen Centre Detection

The Distance Map was used to identify the center line of the lumen inside the artery. The row with the maximum intensity in every column of the distance map, corresponds to the center of the lumen *(center of the black portion is maximally far apart from the nearest white pixel in any direction).* The Lumen Center line is the line joining the brightest pixel in each column of

the Distance Map. The Lumen Width is twice the maximum value (center line value) of the distance map in each column of the image.

***'The intensity value of the Distance Map at the peak intensity location is equal to half of the Lumen Width in that column of the image.'***

*Example:*

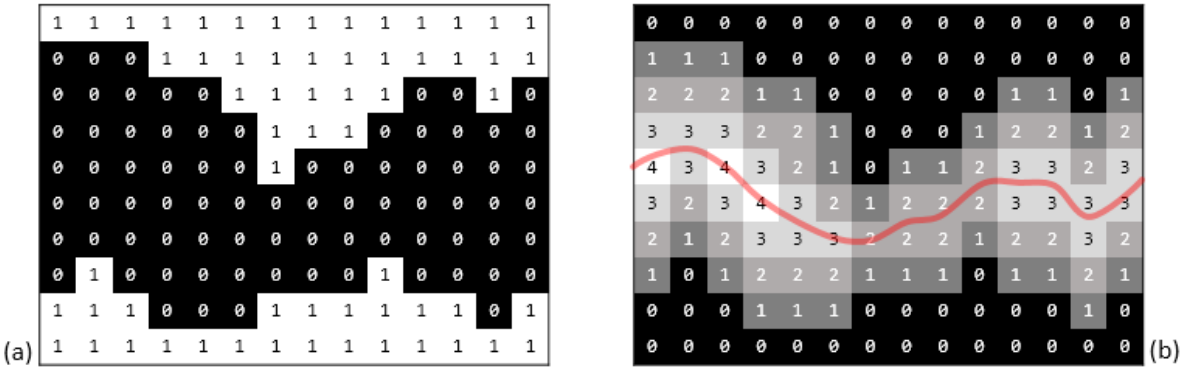


**Figure 2.27:** (a) Threshold Image (b) Distance Map showing Lumen Centre location and intensity values.

### 2.7.4 Bounded Distance Map

The bounded threshold image was used to generate the bounded ***Distance Map***. It was used to determine the lumen width for every column of the image.

The distance mapping could be performed on the unbounded threshold image shown in Figure 38 but the algorithm can bias the peak intensity value of lumen center outside the artery as well that can lead to inaccuracy of the algorithm.

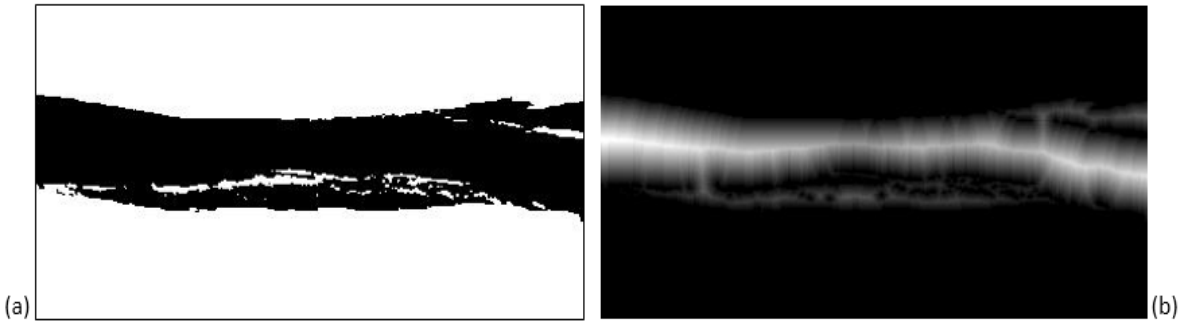


**Figure 2.28:** (a) Threshold Image (b) Bounded Distance Map.

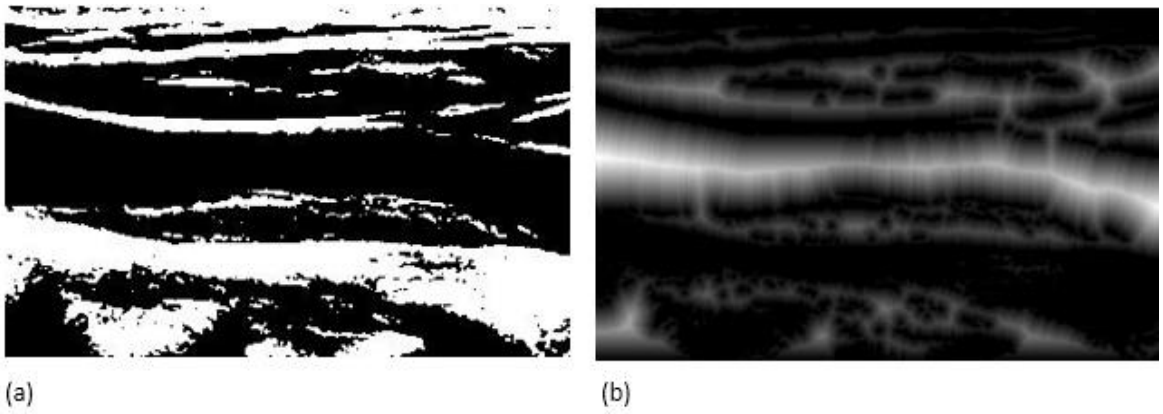


**Figure 2.29:** (a) Unbounded Threshold Image (b)Unbounded Distance Map

## 2.8 Carotid Artery Stenosis Measurement

The percentage Stenosis in one column was given by the following equation(Loizou, 2005)

$$Sten._{CCA} = \left(1 - \frac{W_{Lumen}}{W_{Artery}}\right) \times 100 \qquad (8.1)$$

The Lumen Width in a column was given by;

$$W_{Lumen} = 2 * I_{LumenCenter} - [mod(n_{LumenPixels}, 2)] \qquad (8.2)$$

$I_{LumenCenter}$; is the intensity of the Lumen Center in the Bounded Distance Map

$mod(n_{LumenPixels}, 2)$; checks if the number of pixels of the Lumen in the column are even or odd.

The modulus operator divides the number of pixels in a column by 2 and gives the remainder as 1 (indicating that number of pixels in column are odd) or 0 (indicating that number of pixels in column are even).

The Artery Width in every column is given by;

$$W_{Artery} = \left\| y_{Artery\ Up} - y_{Artery\ Down} \right\| \qquad (8.3)$$

This is essentially the absolute value of the difference in the row numbers of the upper and lower ***Artery Walls***.

Thus the complete formula for calculating the CCA Stenosis in every single column of the image is:

$$Sten._{CCA} = \left[1 - \frac{2*I_{LumenCenter} - mod(n_{LumenPixels},2)}{\left\| y_{Artery\ Up} - y_{Artery\ Down} \right\|}\right] \times 100$$

*(8.4)*

# Chapter 3: BENEFITS AND LIMITATIONS

## 3.1 Benefits

- The automatic stenosis measurement algorithm determines the percentage stenosis in all columns of the image, not just the maximum value.
- This algorithm can be ported to all live ultrasound machines; after initial calibration it can be used on any ultrasound display.
- This algorithm is fully automatic and requires no human input during operation.
- Since this algorithm is fully automatic, it can detect some stenosis cases, which can go undetected by semi-automatic or manual techniques.

## 3.2 Limitations

Every algorithm, being beneficial has some limitations. This algorithm, instead of being automatic, has some requirements and possesses few limitations.

- Insonation Plane should be perpendicular to the carotid artery.
- At least 70% of the artery walls should be visible in the image
- Images should be of the Common Carotid Artery, before bifurcation.
- The artery should be nearly horizontal throughout the image (±5pixel band can be changed but the overall accuracy will be compromised).

## 3.3 Medical Aspects

The proposed algorithm will be a great help in medical imaging by providing assistance to the radiologists in hospitals to accurately determine the percentage carotid artery stenosis in less time only by porting the algorithm to the ultrasound machine. This algorithm will not require the need of manual intervention that will reduce the human errors.

# Chapter 4: RESULTS AND DISCUSSION

## 4.1 Results

Ultrasound images of carotid artery contains a valuable information leading to the measurement of percentage stenosis that is helpful in assessing the presence of stroke and its timely management. The presence of speckle noise, artifacts, acoustic shadowing and manual interpretation are susceptible to human variability and errors. To overcome this issue, a fully automated carotid artery stenosis measurement algorithm was proposed and was tested on dataset of 26 ultrasound images (11 normal and 15 diseased).

A whole scheme of proposed algorithm is pictorially presented in the following images. Figure 39 (a) a shows one of the original B-mode grayscale ultrasound image of carotid artery. Figure 39 (b) shows binary image using local thresholding, the images can be prevented from the effects of contrast or brightness that, in turn, reduces salt and pepper noise in the image without applying median filter. Figure 40 (a) & (b) shows the "Up Lines Image" and "Down Lines Image" containing detected up and down edges/lines form threshold image through image segmentation. The red and blue color is intentionally given to white pixels for the sake of differentiation. Both up and down edges are detected separately, as the Figure 41 shows both edges of the whole image but one cannot differentiate between up and down edges. These edges are then checked pairwise by algorithm for finding the possible "Artery Width". The bounded rows containing up and down edges which are good candidates for "Artery Walls" are indicated in Figure 42 (a) & (b). The final upper and lower artery walls constructed from edges are shown in Figure 43 (a) & (b). We used these artery walls to bound the threshold image so that distance mapping can only be performed within the bounded artery giving the lumen center as peak intensity values and its location shown in Figure 44. Bounding the threshold image is a major advantage of this algorithm that make it superior to other approaches in which artery walls and plaque boundaries detection was done with the expertise of user leading to inaccurate results. By automatically bounding the artery, this algorithm requires no manual intervention. The plot shown in Figure 45 indicates the region of plaque and artery width. The percentage stenosis in each column of the image can be given by the ratio of plaque and artery width, which brings us to another advantage of algorithm as, in manual measurement method, the percentage stenosis can only be measured at a single level of maximum plaque area while in this algorithm it can be measured in each column of the whole image. All the results were verified by comparing them with the manual measurement and one of them is shown in Figure 47. It can

be observed that there is no major difference between manual and automatic segmentation which shows the effectiveness of our approach.

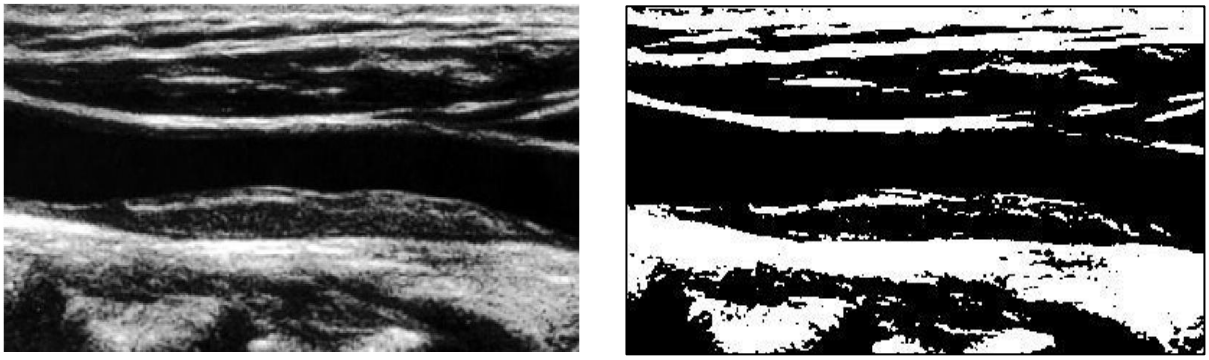

(a) (b)

**Figure 4.1:** (a) Original B-mode grayscale carotid artery ultrasound image (b) Threshold image.

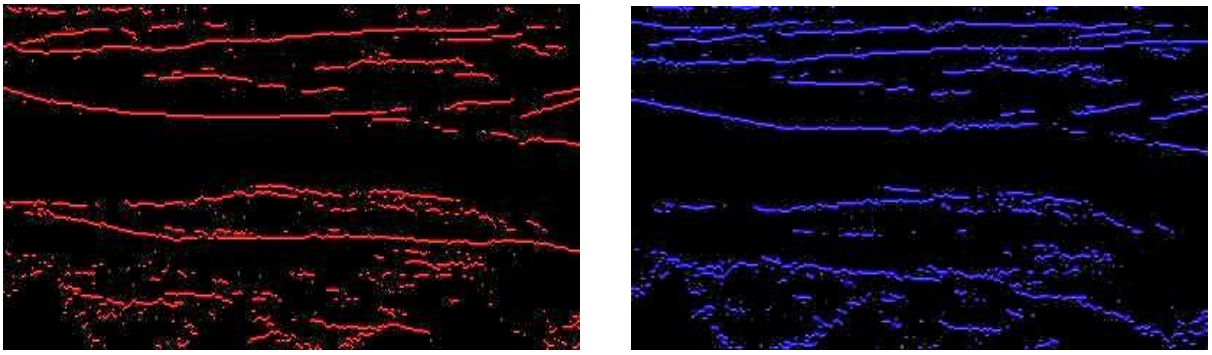

(a) (b)

**Figure 4.2:** (a) Up Lines Image (b) Down Lines Image.

**Figure 4.3:** Detected Up and Down edges.

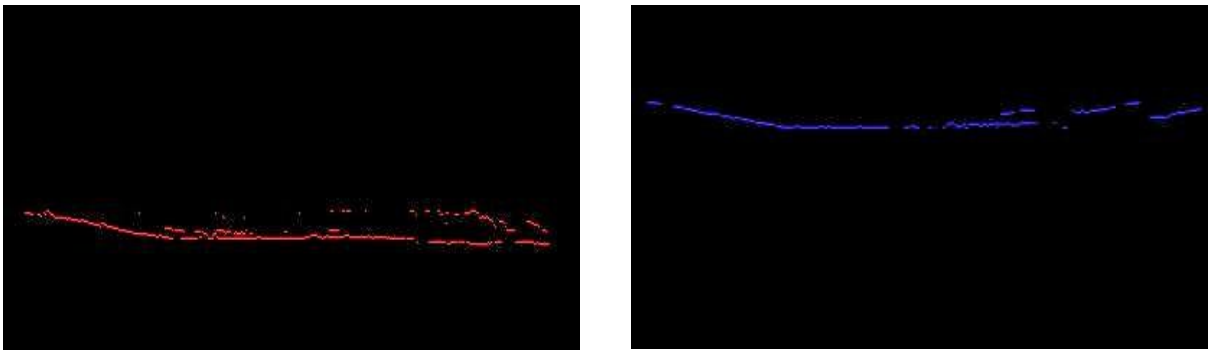

(a) (b)

**Figure 4.4:** (a) Lower Artery wall (Upper-Edges) (b) Upper Artery Wall (Lower-Edges).

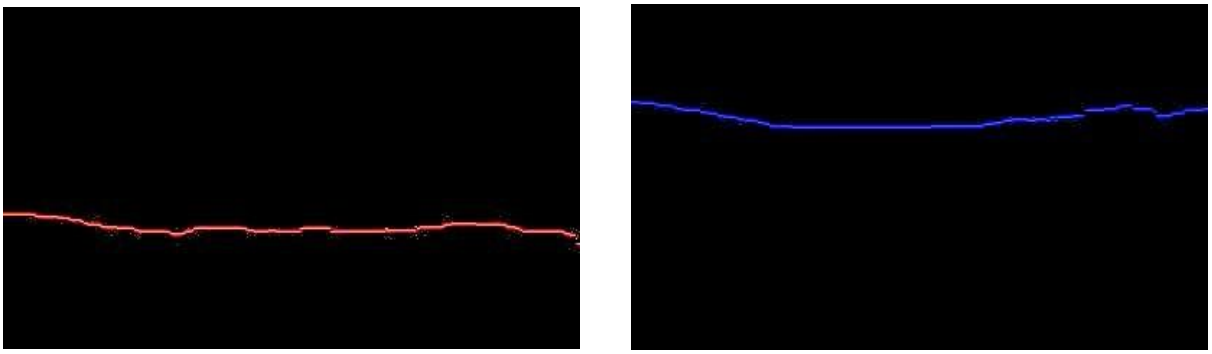

(a) (b)

**Figure 4.5:** (a) Lower Artery Wall (b) Upper Artery Wall.

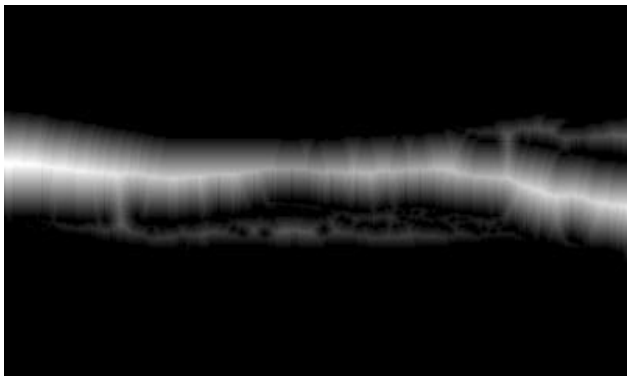

**Figure 4.6:** Bounded Distance Map.

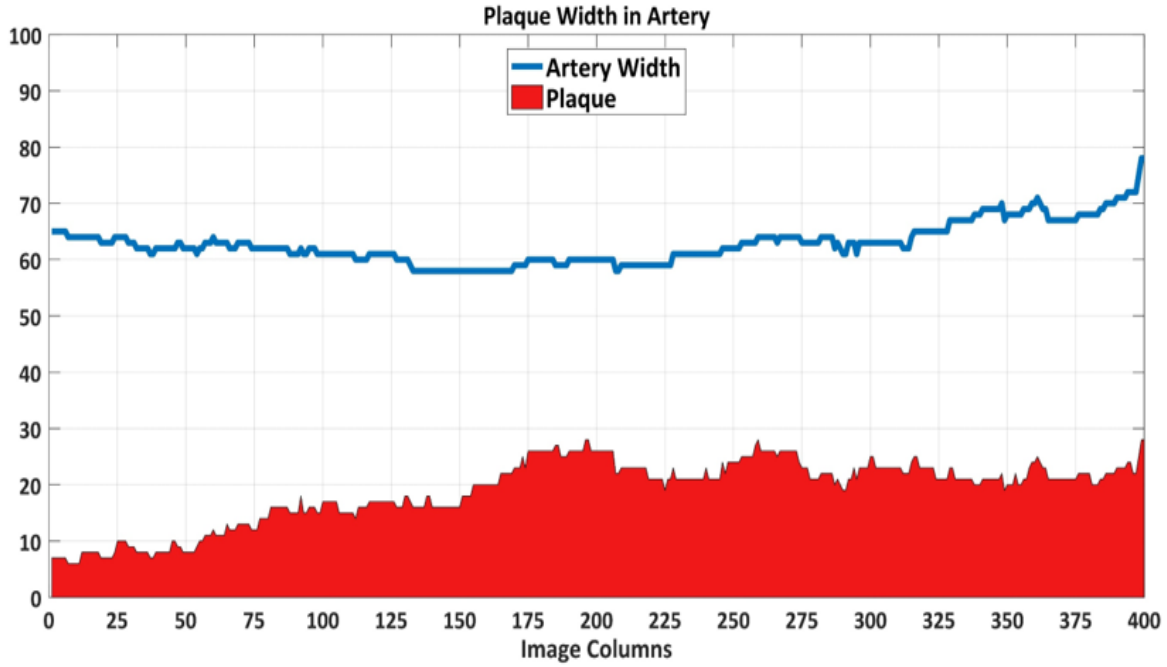


**Figure 4.7:** Plot of Image Columns Vs Plaque Width in Artery.

* Red area indicates the plaque present in the artery and blue line indicates Artery Width.

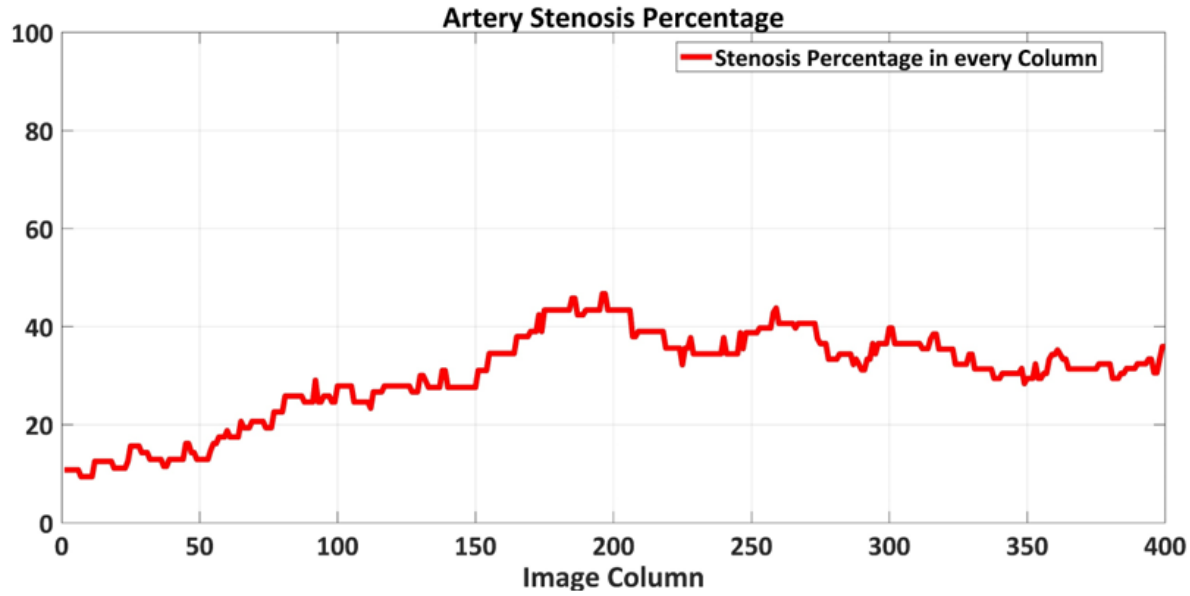


**Figure 4.8:** Plot of Image Column Vs Artery Stenosis Percentage.

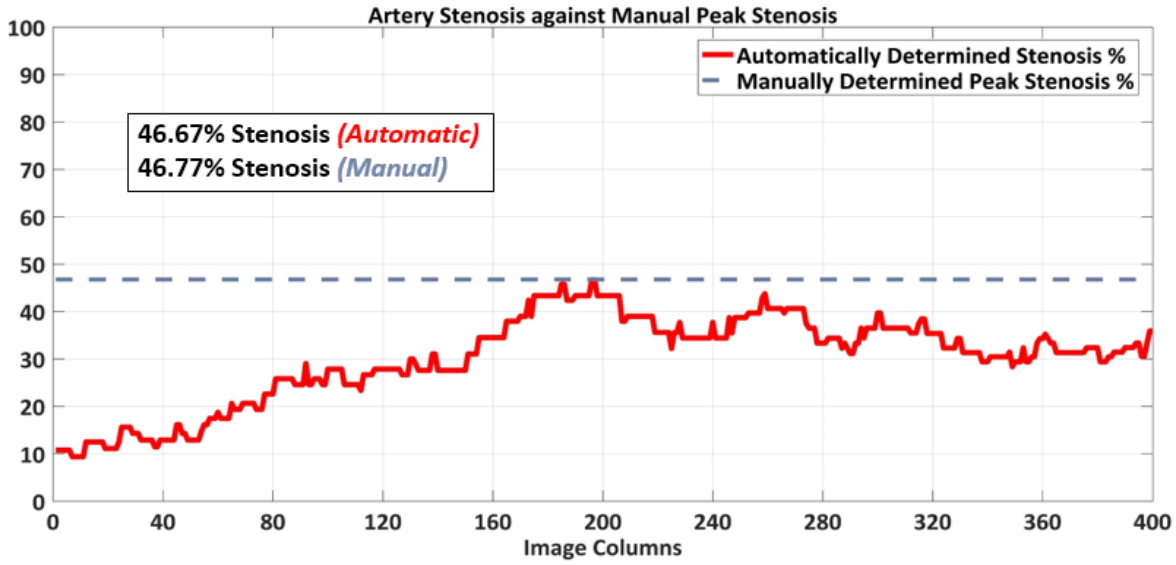


**Figure 4.9:** Comparison of manual and automatic carotid artery stenosis measurement.

### 4.1.1 Statistical Data Analysis

The detection of plaque and lumen are analyzed as separate parameters for the performance of this algorithm given by accuracy, sensitivity, specificity, precision and F1 score.

| Parameter | Lumen | Plaque |
|---|---|---|
| True Positives | 25 | 9 |
| False Positives | 0 | 2 |
| True Negatives | 0 | 9 |
| False Negatives | 1 | 6 |
| Accuracy | 0.9615 | 0.6923 |
| Precision | 1.0 | 0.8182 |
| Sensitivity | 0.9615 | 0.6 |
| Specificity | --- | 0.8182 |
| F1 Score | 0.9804 | 0.6923 |

**Table 4.1:** Statistical analysis of data.

$$Positive\ likelihood\ ratio = \frac{Sensitivity}{1-Specificity} \quad (3.3)$$

$$Negative\ Likelihood\ ratio = \frac{1-Sensitivity}{Specificity} \quad (3.4)$$

The data was verified by comparing it with the results of manual measurement. The number of true positive, true negative, false positive and false negative for lumen and plaque shown in Table 3 & 4 was used to calculate accuracy, precision, sensitivity, specificity and F1 score. It can be observed that the accuracy of algorithm for lumen detection is 96 % while for plaque detection is 69 %. The Precision for lumen detection is 100 % and 81.82 % for plaque detection. The sensitivity of algorithm for lumen and plaque detection is 96 % and 60 % respectively. The Specificity for plaque detection is 81.82 % while the F1 score for lumen detection is 98 % and that for plaque detection is 69.2 %. The positive likelihood ratio for plaque is 3.3 while negative likelihood ratio is 0.26.

The accuracy of a study done by José Rouco et al. (2016) for artery centerline detection was 80% while the 96.15% accuracy can be observed in our proposed algorithm (Rouco et al., 2016). Another study for lumen detection done by André Miguel F.Santos et al. (2013) shows accuracy of 96.78% but the manual segmentation of images by specialist made this algorithm semi-automated and error prone while the accuracy achieved through our algorithm is 96.15% with no involvement of manual interpretation (Santos et al., 2013).

The Algorithm was tested on a number of images and few results are shown below:

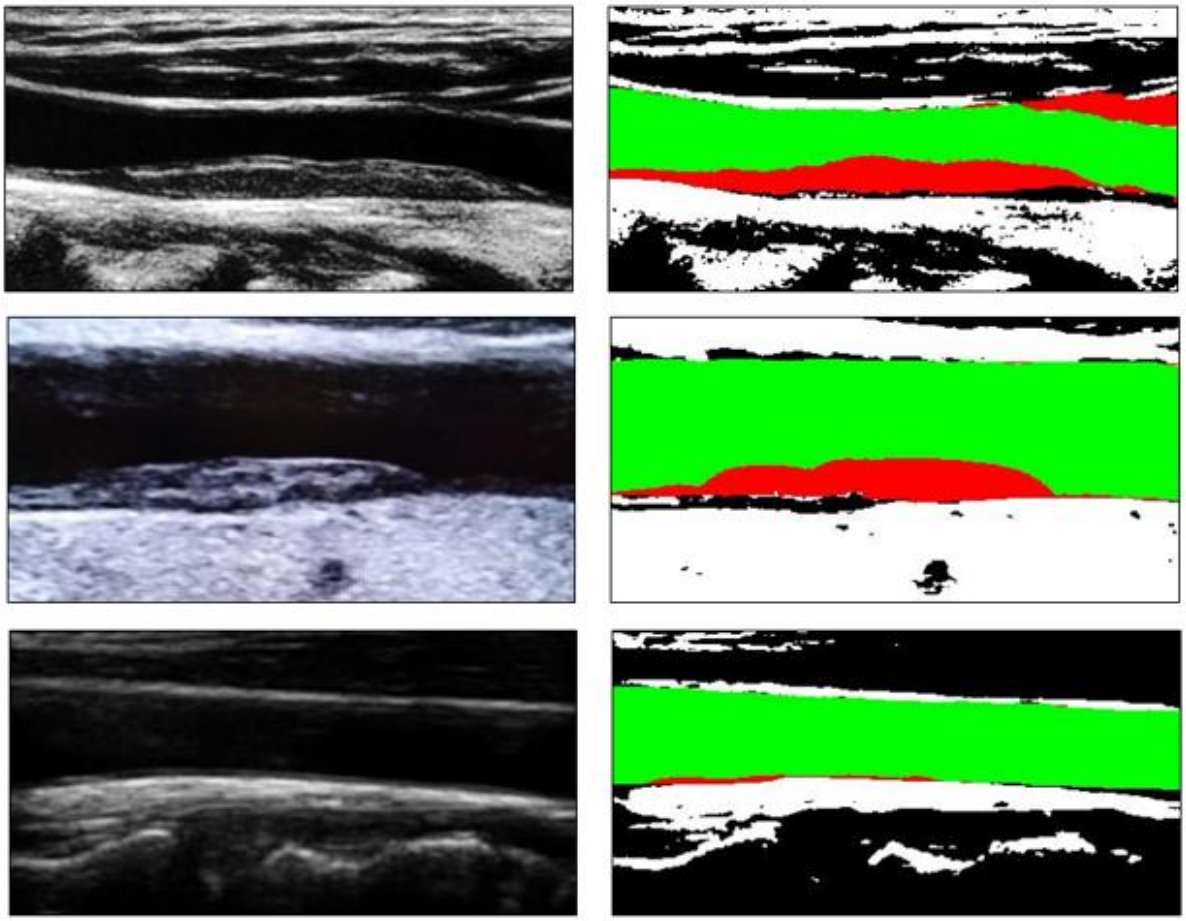

**Figure 4.10:** Original B-mode grayscale images and their Resultant images detected lumen (green) and plaque (red).

Graphical representation of true positive and false negative for automatic Vs manual detection of lumen is shown in Table 3.

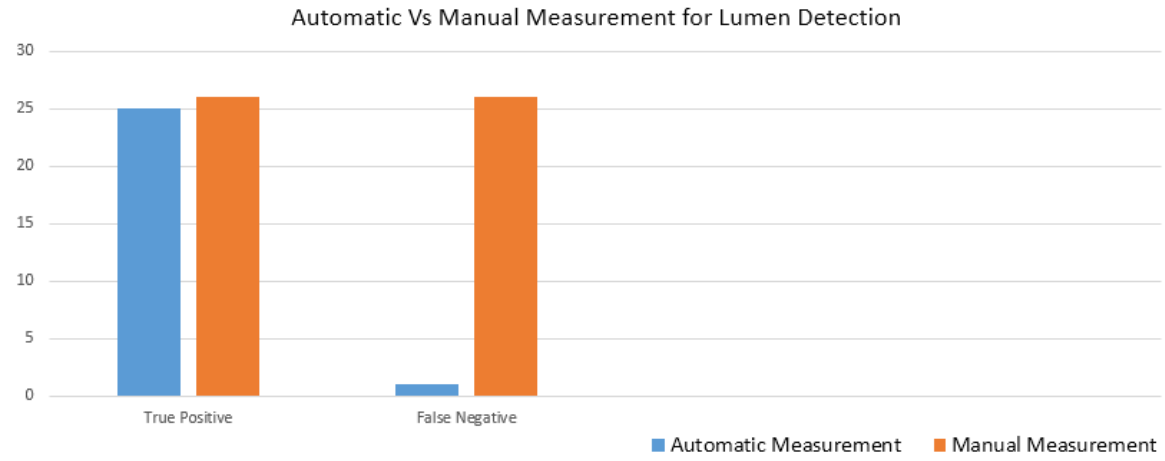


**Table 4.2:** Bar Graph showing automatic Vs manual measurement for lumen detection.

Graphical representation of true positive, true negative, false positive and false negative for automatic Vs manual detection of plaque is shown in Table 4.

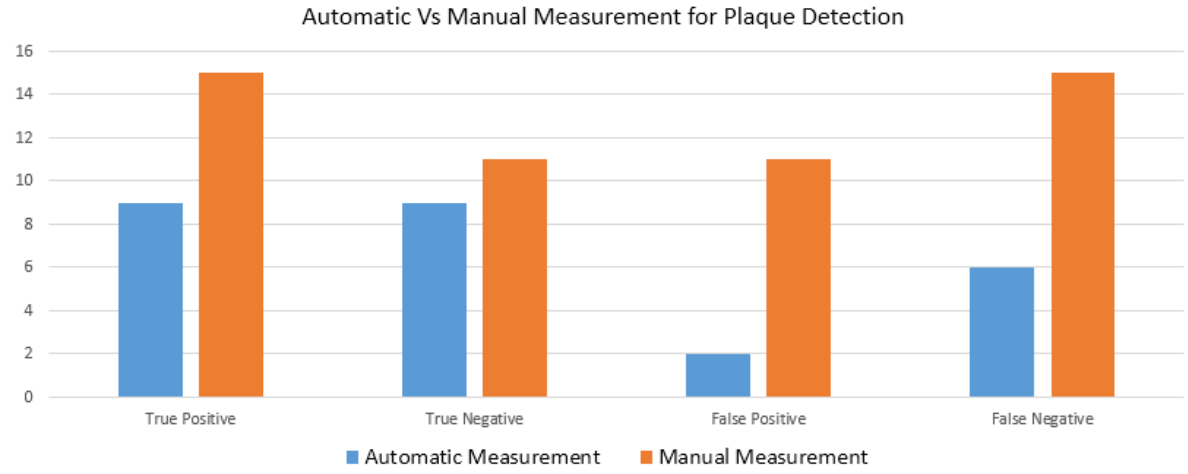


**Table 4.3:** Bar Graph showing automatic Vs manual measurement for plaque detection.

## 4.2 Discussion

Medical image processing is used for automating the different medical procedures for diagnosis and timely management of disease. In this research, an automatic algorithm was implemented for measurement of carotid artery stenosis. The algorithm consists of two important parts that are artery wall detection and lumen width detection through distance map. In the previous studies, selection of Region of Interest (ROI) containing artery wall and plaque boundaries was done manually by medical experts leading to inaccuracy. Our proposed algorithm requires no manual intervention as artery walls were detected automatically and used to bound threshold image to create a bounded distance map giving 96% accuracy for lumen detection and 69.2% for plaque detection. Furthermore, the number of true positive and true negative are greater than the false positive and false negative so, our algorithm is accurate in detecting lumen and plaque giving accurate percentage stenosis. The sensitivity and specificity is calculated for checking the usefulness and correct testing by the algorithm. Sensitivity of algorithm for lumen detection was greater than that for plaque detection. The positive likelihood ratio of greater than one and negative likelihood ratio of less than one indicates correct results. The proposed algorithm can be ported to all live ultrasound machines and can be used by radiologists in hospital that will lead to less tedious procedure and accurate results.

# Chapter 5: CONCLUSION AND RECOMMENDATIONS

## 5.1 Conclusion

The objective of this research was to develop a fully automated carotid artery stenosis measurement algorithm using image segmentation with the two important steps which were artery wall detection and lumen width detection. To the best of our knowledge, many image segmentation techniques have been developed for automation purpose but such an algorithm has not yet been proposed in which percentage stenosis can be measured in each column of the image and without the involvement of medical expert that provided accurate results. The results were compared with those obtained from manual measurement method. The proposed algorithm showed promising results in detection of lumen through bounded distance map while improvement is required in artery wall detection algorithm that will make the plaque detection accurate. The validity measures used to calculate the effectiveness of the algorithm that gives 96% accuracy in lumen detection and 69% accuracy in plaque detection.

## 5.2 Future Recommendations

- Active Contours or Spline Interpolation techniques can be used to improve the artery wall enhancement section.
- Transverse Scan Images can be used with a radial model, instead of a horizontal model.
- Automatic realignment can be added to the image acquisition to ensure horizontal alignment.
- Bifurcation can be treated with a modified integrated artery model.
- A large dataset can be acquired and percentage stenosis can be measured through machine learning and can be deployed on a live ultrasound machine.

# Chapter 6: REFERENCES


Abolmaesumi, P., Sirouspour, M. R., & Salcudean, S. E. (2000). Real-time extraction of carotid artery contours from ultrasound images. In *Computer-Based Medical Systems, 2000. CBMS 2000. Proceedings. 13th IEEE Symposium on* (pp. 181–186). IEEE.

Acharya, U. R., Mookiah, M. R. K., Vinitha Sree, S., Afonso, D., Sanches, J., Shafique, S., … Suri, J. S. (2013). Atherosclerotic plaque tissue characterization in 2D ultrasound longitudinal carotid scans for automated classification: A paradigm for stroke risk assessment. *Medical and Biological Engineering and Computing*, *51*(5), 513–523. https://doi.org/10.1007/s11517-012-1019-0

Bhuiyan, A. R., Srinivasan, S. R., Chen, W., Paul, T. K., & Berenson, G. S. (2006). Correlates of vascular structure and function measures in asymptomatic young adults: The Bogalusa Heart Study. *Atherosclerosis*, *189*(1), 1–7. https://doi.org/10.1016/j.atherosclerosis.2006.02.011

Boussel, L., Serusclat, A., Skilton, M. R., Vincent, F., Bernard, S., Moulin, P., … Douek, P. C. (2007). The Reliability of High Resolution MRI in the Measurement of Early Stage Carotid Wall Thickening. *Journal of Cardiovascular Magnetic Resonance*, *9*(5), 771–776. https://doi.org/10.1080/10976640701544746

Chaudhry, A., Hassan, M., Khan, A., & Kim, J. Y. (2013). Automatic active contour-based segmentation and classification of carotid artery ultrasound images. *Journal of Digital Imaging*, *26*(6), 1071–1081. https://doi.org/10.1007/s10278-012-9566-3

Christodoulou, C. I., Pattichis, C. S., Pantziaris, M., & Nicolaides, A. (2003). Texture-based classification of atherosclerotic carotid plaques. *IEEE Transactions on Medical Imaging*, *22*(7), 902–912.

Christodoulou, L., Loizou, C. P., Spyrou, C., Kasparis, T., & Pantziaris, M. (2012a). FULL-AUTOMATED SYSTEM FOR THE SEGMENTATION Cyprus Institute of Neurology and Genetics, (May), 2–4.

Christodoulou, L., Loizou, C. P., Spyrou, C., Kasparis, T., & Pantziaris, M. (2012b). Full-automated system for the segmentation of the common carotid artery in ultrasound images. In *Communications Control and Signal Processing (ISCCSP), 2012 5th International Symposium on* (pp. 1–6). IEEE.

Committee, N. A. S. C. E. T. S. (1991). North America Symptomatic Carotid Endarterectomy Trial: methods, patient characteristics and progress. *Stroke*, *22*, 711–720.

Delsanto, S., Molinari, F., Liboni, W., Giustetto, P., Badalamenti, S., & Suri, J. S. (2006). User-independent plaque characterization and accurate IMT measurement of carotid artery wall using ultrasound. In *Engineering in Medicine and Biology Society, 2006. EMBS'06. 28th Annual International Conference of the IEEE* (pp. 2404–2407). IEEE.

Dis, S. C. (1995). Carotid endarterectomy for patients with asymptomatic internal carotid artery stenosis. *Journal of Stroke and Cerebrovascular Diseases*, *5*(1), 56–57. https://doi.org/10.1016/S1052-3057(10)80088-6

El-Barghouty, N., Nicolaides, A., Bahal, V., Geroulakos, G., & Androulakis, A. (1996). The identification of the high risk carotid plaque. *European Journal of Vascular and Endovascular Surgery*, *11*(4), 470–478.

Fernhall, B., & Agiovlasitis, S. (2008). Arterial function in youth: window into cardiovascular risk. *Journal of Applied Physiology*, *105*(1), 325–333.

Fetics, B. J., Wong, E. Y., Murabayashi, T., Nelson, G. S., Cohen, M.-M., Rochitte, C. E., … Nevo, E. (2001). Enhancement of contrast echocardiography by image variability analysis. *IEEE Transactions on Medical Imaging*, *20*(11), 1123–1130.

Geroulakos, G., Hobson, R. W., & Nicolaides, A. N. (1996). Ultrasonic carotid plaque morphology. *JEMU-PARIS-*, *17*, 165–170.

Gill, J. D., Ladak, H. M., Steinman, D. A., & Fenster, A. (1999). Development and evaluation of a semiautomatic 3D segmentation technique of the carotid arteries from 3D ultrasound images. In *Medical Imaging 1999: Image Processing* (Vol. 3661, pp. 214–222). International Society for Optics and Photonics.

Gill, J. D., Ladak, H. M., Steinman, D. A., & Fenster, A. (2000). Accuracy and variability assessment of a semiautomatic technique for segmentation of the carotid arteries from three-dimensional ultrasound images. *Medical Physics*, *27*(6), 1333–1342.

Gill, J. D., Ladak, H. M., Steinman, D. A., & Fenster, A. (2000). Segmentation of ulcerated plaque: A semi-automatic method for tracking the progression of carotid atherosclerosis. In *Engineering in Medicine and Biology Society, 2000. Proceedings of the 22nd Annual International Conference of the IEEE* (Vol. 1, pp. 669–672). IEEE.

Gustavsson, T., Abu-Gharbieh, R., Hamarneh, G., & Liang, Q. (1997). Implementation and comparison of four different boundary detection algorithms for quantitative ultrasonic measurements of the human carotid artery. In *Computers in Cardiology 1997* (pp. 69–72). IEEE.

Gutierrez, M. A., Pilon, P. E., Lage, S. G., Kopel, L., Carvalho, R. T., & Furuie, S. S. (2002). Automatic measurement of carotid diameter and wall thickness in ultrasound images. In *Computers in Cardiology, 2002* (pp. 359–362). IEEE.

Gutstein, D. E., & Fuster, V. (1999). Pathophysiology and clinical significance of atherosclerotic plaque rupture. *Cardiovascular Research, 41*(2), 323–333.

Hamou, A. K., & El-Sakka, M. R. (2004). A novel segmentation technique for carotid ultrasound images. In *Acoustics, Speech, and Signal Processing, 2004. Proceedings.(ICASSP'04). IEEE International Conference on* (Vol. 3, p. iii-521). IEEE.

Johnson, J. M., Kennelly, M. M., Decesare, D., Morgan, S., & Sparrow, A. (1985). Natural history of asymptomatic carotid plaque. *Archives of Surgery, 120*(9), 1010–1012.

Ladak, H. M., Milner, J. S., & Steinman, D. A. (2000). Rapid three-dimensional segmentation of the carotid bifurcation from serial MR images. *Journal of Biomechanical Engineering, 122*(1), 96–99.

Ladak, H. M., Thomas, J. B., Mitchell, J. R., Rutt, B. K., & Steinman, D. A. (2001). A semi-automatic technique for measurement of arterial wall from black blood MRI. *Medical Physics, 28*(6), 1098–1107.

Liang, Q., Wendelhag, I., Wikstrand, J., & Gustavsson, T. (2000). A multiscale dynamic programming procedure for boundary detection in ultrasonic artery images. *IEEE Transactions on Medical Imaging, 19*(2), 127–142.

Liu, L., Zhao, F., Yang, Y., Qi, L. T., Zhang, B. W., Chen, F., … Liu, L. S. (2008). The clinical significance of carotid intima-media thickness in cardiovascular diseases: A survey in Beijing. *Journal of Human Hypertension, 22*(4), 259–265. https://doi.org/10.1038/sj.jhh.1002301

Loizou, C. P. (2005). Ultrasound image analysis of the carotid artery, (October). Retrieved from http://ethos.bl.uk/OrderDetails.do?did=1&uin=uk.bl.ethos.555041

Loizou, C. P. (2014). A review of ultrasound common carotid artery image and video segmentation techniques. *Medical & Biological Engineering & Computing*, *52*(12), 1073–1093. https://doi.org/10.1007/s11517-014-1203-5

Loizou, C. P., Kasparis, T., Spyrou, C., & Pantziaris, M. (2013). Integrated system for the complete segmentation of the common carotid artery bifurcation in ultrasound images. In *IFIP International Conference on Artificial Intelligence Applications and Innovations* (pp. 292–301). Springer.

Mao, F., Gill, J., Downey, D., & Fenster, A. (2000). Segmentation of carotid artery in ultrasound images: Method development and evaluation technique. *Medical Physics*, *27*(8), 1961–1970.

Middleton, I., & Damper, R. I. (2004). Segmentation of magnetic resonance images using a combination of neural networks and active contour models. *Medical Engineering & Physics*, *26*(1), 71–86.

Molinari, F., Zeng, G., & Suri, J. S. (2010a). A state of the art review on intima-media thickness (IMT) measurement and wall segmentation techniques for carotid ultrasound. *Computer Methods and Programs in Biomedicine*, *100*(3), 201–221. https://doi.org/10.1016/j.cmpb.2010.04.007

Molinari, F., Zeng, G., & Suri, J. S. (2010b). An integrated approach to computer-based automated tracing and its validation for 200 common carotid arterial wall ultrasound images: A new technique. *Journal of Ultrasound in Medicine*, *29*(3), 399–418.

Naik, V., Gamad, R. S., & Bansod, P. P. (2013). Carotid artery segmentation in ultrasound images and measurement of intima-media thickness. *BioMed Research International*, *2013*. https://doi.org/10.1155/2013/801962

Nicolaides, A. N., Kakkos, S. K., Griffin, M., Geroulakos, G., & Bashardi, E. (2002). Ultrasound plaque characterisation, genetic markers and risks. *Pathophysiology of Haemostasis and Thrombosis*, *32*(5–6), 371–377.

Nicolaides, A., Sabetai, M., Kakkos, S. K., Dhanjil, S., Tegos, T., Stevens, J. M., … Geroulakos, G. (2003). The asymptomatic carotid stenosis and risk of stroke (ACSRS) study. *Int Angiol*, *22*(3), 263–272.

Roman, M. J., Naqvi, T. Z., Gardin, J. M., Gerhard-Herman, M., Jaff, M., & Mohler, E. (2006).

American society of echocardiography report. Clinical application of noninvasive vascular ultrasound in cardiovascular risk stratification: a report from the American Society of Echocardiography and the Society for Vascular Medicine and Biology. *Vascular Medicine (London, England)*, *11*(3), 201–211. Retrieved from http://www.ncbi.nlm.nih.gov/pubmed/17288128

Rothwell, P. M., Gibson, R. J., Slattery, J., Sellar, R. J., Warlow, C. P., & Carotid, E. (1994). Equivalence of Measurements of Carotid Stenosis. *American Heart Association*, 2435–2439.

Rothwell, P. M., & Goldstein, L. B. (1995). Carotid endarterectomy for asymptomatic carotid stenosis. The Asymptomatic Carotid Surgery (ACAS) Trial. *JAMA*, *273*, 1421–1428.

Rouco, J., Azevedo, E., & Campilho, A. (2016). Automatic lumen detection on longitudinal ultrasound b-mode images of the carotid using phase symmetry. *Sensors*, *16*(3), 350.

Santos, A. M. F., Dos Santos, R. M., Castro, P. M. A. C., Azevedo, E., Sousa, L., & Tavares, J. M. R. S. (2013). A novel automatic algorithm for the segmentation of the lumen of the carotid artery in ultrasound B-mode images. *Expert Systems with Applications*, *40*(16), 6570–6579.

Schargrodsky, H., Hernández-Hernández, R., Champagne, B. M., Silva, H., Vinueza, R., Silva Ayçaguer, L. C., … Wilson, E. (2008). CARMELA: Assessment of Cardiovascular Risk in Seven Latin American Cities. *American Journal of Medicine*, *121*(1), 58–65. https://doi.org/10.1016/j.amjmed.2007.08.038

Touboul, P. J., Hennerici, M. G., Meairs, S., Adams, H., Amarenco, P., Bornstein, N., … Zureik, M. (2007). Mannheim carotid intima-media thickness consensus (2004-2006): An update on behalf of the advisory board of the 3rd and 4th Watching the Risk Symposium 13th and 15th European Stroke Conferences, Mannheim, Germany, 2004, and Brussels, Belgium, 2006. *Cerebrovascular Diseases*, *23*(1), 75–80. https://doi.org/10.1159/000097034

Touboul, P. J., Hernández-Hernández, R., Küçükoğlu, S., Woo, K. S., Vicaut, E., Labreuche, J., … Vinueza, R. (2007). Carotid artery intima media thickness, plaque and framingham cardiovascular score in Asia, Africa/Middle East and Latin America: The PARC-AALA Study. *International Journal of Cardiovascular Imaging*, *23*(5), 557–567. https://doi.org/10.1007/s10554-006-9197-1

Watanabe, H., Yamane, K., Egusa, G., & Kohno, N. (2004). Influence of westernization of lifestyle on the progression of IMT in Japanese. *Journal of Atherosclerosis and Thrombosis*, *11*(6), 330–334. https://doi.org/JST.JSTAGE/jat/11.330 [pii]

Wendelhag, I., Liang, Q., Gustavsson, T., & Wikstrand, J. (1997). A new automated computerized analyzing system simplifies readings and reduces the variability in ultrasound measurement of intima-media thickness. *Stroke*, *28*(11), 2195–2200.

Wilhjelm, J. E., Gronholdt, M.-L., Wiebe, B., Jespersen, S. K., Hansen, L. K., & Sillesen, H. (1998). Quantitative analysis of ultrasound B-mode images of carotid atherosclerotic plaque: correlation with visual classification and histological examination. *IEEE Transactions on Medical Imaging*, *17*(6), 910–922.

Yang, X., Ding, M., Lou, L., Yuchi, M., Qiu, W., & Sun, Y. (2011). Common carotid artery lumen segmentation in B-mode ultrasound transverse view images. *International Journal of Image, Graphics and Signal Processing (IJIGSP)*, *3*(5), 15.

Zahalka, A., & Fenster, A. (2001). An automated segmentation method for three-dimensional carotid ultrasound images. *Physics in Medicine & Biology*, *46*(4), 1321.

Zarins, C. K., Xu, C., & Glagov, S. (2001). Atherosclerotic enlargement of the human abdominal aorta. *Atherosclerosis*, *155*(1), 157–164. https://doi.org/10.1016/S0021-9150(00)00527-X